HHS Public Access

Author manuscript

Dev Biol. Author manuscript; available in PMC 2017 December 01.

Published in final edited form as:

Dev Biol. 2016 December 1; 420(1): 148–165. doi:10.1016/j.ydbio.2016.09.019.

Cerebrovascular defects in *Foxc1* mutants correlate with aberrant WNT and VEGF-A pathways downstream of retinoic acid from the meninges

Swati Mishra[a], **Youngshik Choe**[b,1], **Samuel J. Pleasure**[b], and **Julie A. Siegenthaler**[a,*]

[a]Department of Pediatrics, Section of Developmental Biology, University of Colorado, School of Medicine Aurora, CO 80045 USA

[b]Department of Neurology, Programs in Neuroscience and Developmental Biology, Institute for Regenerative Medicine, UC San Francisco, San Francisco, CA 94158 USA

Abstract

Growth and maturation of the cerebrovasculature is a vital event in neocortical development however mechanisms that control cerebrovascular development remain poorly understood. Mutations in or deletions that include the *FOXC1* gene are associated with congenital cerebrovascular anomalies and increased stroke risk in patients. *Foxc1* mutant mice display severe cerebrovascular hemorrhage at late gestational ages. While these data demonstrate Foxc1 is required for cerebrovascular development, its broad expression in the brain vasculature combined with *Foxc1* mutant's complex developmental defects have made it difficult to pinpoint its function(s). Using global and conditional *Foxc1* mutants, we find 1) significant cerebrovascular growth defects precede cerebral hemorrhage and 2) expression of Foxc1 in neural crest-derived meninges and brain pericytes, though not endothelial cells, is required for normal cerebrovascular development. We provide evidence that reduced levels of meninges-derived retinoic acid (RA), caused by defects in meninges formation in *Foxc1* mutants, is a major contributing factor to the cerebrovascular growth defects in *Foxc1* mutants. We provide data that suggests that meninges-derived RA ensures adequate growth of the neocortical vasculature via regulating expression of WNT pathway proteins and neural progenitor derived-VEGF-A. Our findings offer the first evidence for a role of the meninges in brain vascular development and provide new insight into potential causes of cerebrovascular defects in patients with *FOXC1* mutations.

Keywords

Foxc1; cerebrovascular development; WNT; VEGF; meninges; endothelial cell

[*]Corresponding Author: Julie A. Siegenthaler, PhD, University of Colorado, School of Medicine, Department of Pediatrics, 12800 East 19th Ave MS-8313, Aurora, CO 80045 USA, Telephone #: 303-724-3123. julie.siegenthaler@ucdenver.edu.

[1]Current Address: Department of Neural Development and Disease, Korea Brain Research Institute, Daegu, 701-300 Korea.

Introduction

Development of the neocortex requires significant metabolic activity, supported by an extensive vascular plexus that forms concurrent with corticogenesis. Vessel growth and patterning in the developing mouse telencephalon, which includes the neocortex, has a defined, sequential program (Stubbs et al., 2009; Vasudevan et al., 2008). At early stages of embryonic development, mesoderm-derived endothelial cells form a perineural vascular plexus (PNVP) around the brain and spinal cord amongst the forming meninges (Hogan et al., 2004). Blood vessels first appear in the ventral telencephalon and grow in a ventral to dorsal direction within the telencephalic ventricular zone (VZ) where rapidly proliferating neural progenitors reside. This vascular network, known as the periventricular vascular plexus (PVVP), is the first vascular plexus in the developing neocortex and forms between embryonic day 10-11 (E10-11) (Vasudevan et al. 2008). Beginning at ~E12 postmitotic neurons begin to accumulate to form the cortical plate within the neocortex (Molyneaux et al., 2007). At the same time, PNVP-derived vessels begin to enter the cortex at several points along its surface to form a second, more superficial vascular plexus within the cortical plate (Marin-Padilla, 1985; Strong, 1964). Over the course of pre- and postnatal corticogenesis, these two plexuses become largely indistinguishable as they fuse to form an integrated cerebrovascular plexus. Defects in cerebrovascular development can lead to irreparable brain damage thus it is important to understand the cellular and molecular underpinnings of this developmental process.

Foxc1 is a forkhead transcription factor with several functions in embryonic development, including eye, craniofacial and brain development. Severe cerebral hemorrhage has been repeatedly reported in global *Foxc1* knockout mice (Green, 1970; Gruneberg, 1943; Hecht et al., 2010; Siegenthaler et al., 2009) and, recently, vascular growth defects were described in early embryonic ventral telencephalon of *Foxc1* mutants (Prasitsak et al., 2015). However, the role of Foxc1 in cerebrovascular development remains unclear. This is a clinically relevant question as human patients with point mutations or deletions that encompass *FOXC1* have cerebrovascular defects that increase the risk for stroke (French et al., 2014). One of the challenges of identifying Foxc1's function is that it is expressed both by brain endothelial cells that make up the vascular tubes and brain pericytes, a perivascular cell type with key functions in vascular stability and blood-brain barrier (BBB) maturation and maintenance (Armulik et al., 2010; Hellström et al., 2001). Evidence from endothelial and pericyte conditional *Foxc1* mutants, however, suggest that the severe cerebral hemorrhage in global *Foxc1* mutants cannot be solely attributable to Foxc1's function in these two cell types. Mice with endothelial cell-conditional deletion of *Foxc1* live into adulthood suggesting that they do not have severe brain vascular defects (Hayashi and Kume, 2008). Pericyte conditional *Foxc1* mutants have small, focal cerebral hemorrhages and dilated cerebrovasculature indicating that *Foxc1* is required in pericytes for normal vascular morphogenesis (Siegenthaler et al., 2013). However, the cerebrovascular phenotype in pericyte conditional *Foxc1* mutants is much milder that global *Foxc1* knockouts indicating that Foxc1 functions in a different cell type(s) to regulate cerebrovascular development.

Foxc1 is not expressed by any neural cells in the brain but is strongly expressed by meningeal fibroblasts (Siegenthaler et al., 2009; Vivatbutsiri et al., 2008; Zarbalis et al.,

2007). The meninges play several key roles in brain development and Foxc1 is required for meninges function (Aldinger et al., 2009; Haldipur et al., 2015; Haldipur et al., 2014; Hecht et al., 2010; Siegenthaler et al., 2009; Zarbalis et al., 2012; Zarbalis et al., 2007). In the *Foxc1* mutant telencephalon, formation of the neural crest-derived meninges that overlay the neocortex is severely impaired and this results in a reduction of meningeal-derived cues required for normal development of the neocortex (Harrison-Uy and Pleasure, 2012; Hecht et al., 2010; Siegenthaler et al., 2009; Zarbalis et al., 2012; Zarbalis et al., 2007). The reduction in meninges-secreted factors required for corticogenesis, notably retinoic acid (RA), leads to expansion of neocortical progenitors at the expense of generating neocortical neurons (Siegenthaler et al. 2009). What has not been looked at is whether loss of meningeal-derived factors could also negatively impact cerebrovascular development in *Foxc1* mutants.

Here we use a combination of global and conditional mouse mutants to 1) characterize the cerebrovascular defects in *Foxc1* mutants, 2) define which cell types require Foxc1 to regulate cerebrovascular development and 3) identify a previously unknown role for the meninges in this process. Our analysis reveals severe reduction in cerebrovascular growth and diminished endothelial cell proliferation in *Foxc1* mutants prior to cerebral hemorrhage. Further, we show that conditional deletion of *Foxc1* in neural crest derived cells using *Wnt1-Cre*, which includes telencephalic meninges and pericytes, is sufficient to recapitulate the cerebrovascular defects seen in global *Foxc1* knockouts. We provide data that RA from the meninges has an important function in cerebrovascular development, specifically to regulate WNT and VEGF-A pathways and ensure cerebrovascular growth.

Experimental Procedures

Animals

All mice were housed in specific-pathogen-free facilities approved by AALAC and were handled in accordance with protocols approved by the IACUC committee on animal research. The following mouse lines were used in this study: *Foxc1*^{lacZ} (Kume et al., 1998), *Foxc1*^{hith} (Zarbalis et al., 2007), *Pdgfbi-Cre* (Claxton et al., 2008), *Wnt1-Cre* (Brault et al., 2001), *Bat-gal-lacZ* (Maretto et al., 2003), *Ctnnb1-flox* (Brault et al., 2001), dominant negative Retinoic Acid Receptor-α (dnRAR403)-flox (Rosselot et al., 2010), *Tie2-Cre* (Tek-Cre) (Kisanuki et al., 2001), *Rosa26-YFP* (Srinivas et al., 2001) and *Foxc1-flox* (Sasman et al., 2012). *Foxc1*$^{LacZ/+}$ or *Foxc1*$^{hith/+}$male and female mice were interbred to generate *Foxc1*$^{LacZ/LacZ}$ and *Foxc1*$^{hith/hith}$ mutants, respectively and *Foxc1*$^{LacZ/+}$, *Foxc1*$^{hith/+}$, and *Foxc1*$^{+/+}$ littermates were used as controls. *Foxc1*$^{LacZ/+}$ and *Foxc1*$^{hith/+}$ male and female mice were interbred to generate *Foxc1*$^{hith/lacz}$ mutant embryos. Tamoxifen (Sigma) was dissolved in corn oil (Sigma; 20mg/ml) and 100μl was injected intra-peritoneal into pregnant females at E9.5 and E10.5 to generate *Pdgfbi-Cre; dnRAR403-fl/fl* mutant embryos or E11.5 and E12.5 to generate *PdgfbiCre; Ctnnb1-fl/fl* mutant embryos.

Retinoic acid diet

Pregnant dams carrying control and *Foxc1*$^{hith/lacz}$ embryos were fed an all trans-retinoic acid (atRA) enriched diet (200 mg/Kg of food; Harlan Teklab Custom diets) from E10 to E14.5 and sacrificed on E14.5 for harvesting control and mutant tissue.

X-gal staining, immunofluorescence and imaging

Embryos were collected and whole heads of the embryos were fixed overnight with 4% paraformaldehyde. E11.5 embryos for x-gal staining were fixed for 30 min in 4% paraformaldehyde. Adult *Tie2-Cre; Foxc1-flox* animals were injected with a lethal dose of pentobarbital and perfused trans-cardiac with PBS followed by 4% paraformaldehyde. All tissues were cryoprotected with 20% sucrose in PBS and subsequently frozen in OCT. Tissue was cryosectioned in 12μm, 25μm (x-gal staining) or 50μm (GLUT1 immunofluorescence for branchpoint and PNVP-derived vessel analysis) increments. Sections for x-gal staining were incubated overnight in 1 mg/ml x-gal in staining solution (Sigma). Immunohistochemistry was performed on control and mutant tissue sections using the following antibodies: rabbit anti-β-galactosidase 1:500 (Cappel), rabbit anti-GLUT1 1:250 (Lab Vision-Thermo Scientific), rabbit anti- ETS related gene 1 (ERG1) 1:200 (Abcam) and mouse anti-BrdU 1:50 (BD Biosciences), PDGFrβ 1:100 (Cell Signaling Technologies), rat anti-CD31 1:200 (Biosciences), mouse anti-Tuj1 1:500 (Millipore) and rabbit anti-desmin 1:200 (Cell Signaling Technologies). Following incubation with primary antibodies, tissue sections were incubated with appropriate Alexafluor-conjugated secondary antibodies (Invitrogen), Alexafluor 633-conjugated isolectin-B4 1:100 (Invitrogen), and DAPI to label cell nuclei (Invitrogen). Foxc1 immunofluorescence was performed as described previously (Zarbalis et al., 2007). The immunostained tissue sections were imaged using Nikon eclipse i80 with associated NIS elements AR 4.11.00 software for analysis of images and Zeiss 780 LSM with associated Zeiss Zen software.

Quantitative analysis of the cerebrovasculature

Whole head tissue sections were immunostained for GLUT1, enriched in CNS blood vessels, and isolectin-b4 (IB4), expressed by all blood vessels, to analyze changes in blood vessel branch points, vessel diameter, number of blood vessels entering neocortex of E14.5 control, *Foxc1*$^{hith/lacZ}$ (non-treated and atRA treated) and control and *PdgfbiCre; dnRAR403 fl/fl* mutant embryos. For quantification of blood vessel diameter, average diameters of GLUT1+ blood vessels in a 20X image were measured. For analysis of blood vessel density, the sum of IB4+ blood vessels length was divided by the area of the tissue and these values were determined from every 20X image. For quantification of number of vessel branch points, the total number of vessel branches sprouting from all the blood vessels in a given 20X image field were divided by the tissue area analyzed. All vessel diameter, vessel density and vessel branch point measurements were performed using Image J software (NIH) on a minimum of 10, 20X fields per brain. A minimum of three brains per genotype and per treatment were used (n≥3).

Analysis of Bat-gal-lacZ in cerebrovasculature

For quantification of β-gal+ endothelial cells in the neocortical PNVP, the number of β-galactosidase+/IB4+ endothelial cells was counted in 20× image. For quantification of β-gal + endothelial cells in blood vessels within the neocortex, the number of IB4+ blood vessels containing a β-gal+ endothelial cell was divided by the total number of blood vessels within a 20x image. Both analysis were performed on a minimum of 5, 20x fields per brain. A minimum of three brains per genotype and per treatment were used (n≥3).

Endothelial cell proliferation analysis

For analysis of cell proliferation, pregnant dams were injected with BrdU (50 mg/kg b.w.) 2 hours prior to embryo collection. E14.5 brain tissue sections were immunostained for ERG1, which labels endothelial cell nuclei, and BrdU, which labels cells in S-phase, and were used to quantify endothelial cell proliferation in the neocortical or thalamic brain regions. ERG1+/BrdU+ cells were divided by the total number of ERG1+ cells in a 20X image to obtain a labeling index, a measure of cell proliferation. All measurements were performed using ImageJ software (NIH) on a minimum of 10, 20X fields per brain. A minimum of three brains per genotype and per treatment were used (n≥3).

WNT7a/b in situ hybridization

E14.5 control and *Foxc1*$^{hith/LacZ}$ mutant embryos were collected and fixed overnight in 4% paraformaldehyde, processed through 20% sucrose then sectioned in 20 μm increments. Antisense probes for *WNT7a* and *WNT7b* were generated via PCR using forward and reserve primers as reported on the Allen Brain Atlas: Developmental Brain. Sections were processed for ISH as described previously (Choe et al., 2012) and imaged using a Retiga CCD-cooled camera with color filter and associated QCapture Pro software (QImaging Surrey, BC Canada).

Neocortical progenitor cell culture

E14 cortical progenitor cells (R&D systems) were seeded onto 15μg/ml Poly-L-ornithine (Sigma) and 1μg/ml laminin (Sigma) coated 6 well plates as a monolayer culture. Cell culture medium was composed of DMEM/F-12 with glutamax (Life Technologies), 1X N2 supplement composed of Insulin, Human Transferrin, Putrescine, Selenite and Progesterone (Life Technologies) and glucose (Sigma). Culture medium was supplemented with 10ng/ml of human basic fibroblast growth factor (R&D systems) and 10ng/ml of human epidermal growth factor (R&D systems) every day until cell lysate collection to maintain cortical progenitors cells in an undifferentiated state.

Neocortical neuron cell culture

E14 cortical progenitor cells (R&D systems) were seeded onto 20μg/ml Poly-L-ornithine (Sigma) and 10μg/ml laminin (Sigma) coated 6 well plates as a monolayer culture. After 2 days, progenitor medium (as described above) was changed to neural differentiation medium which was composed of Neurobasal medium (Stem Cell Technologies), B27 serum free supplement (2%,Life technologies) and GlutaMAX™-I Supplement (2mM Life

technologies). Differentiation medium was changed every 3-4 days and 0.5 mM of dibutyryl cAMP (Sigma) was added starting on day 7 of differentiation for 3 days.

Quantitative Real-time PCR

Total cellular RNA was isolated from two sources 1) control (untreated), hypoxia-exposed ($3\%O_2$), 1μM RA-treated (Sigma) and 1μM RA +1μM pan-Retinoic Acid Receptor antagonist (Santa Cruz Biotechnology) treated E14 mouse cortical progenitor cells plated in 6-well plates or 2) PNVP/meninges isolated from the telencephalon of E14.5 control or *Foxc1*$^{hith/lacZ}$ mutants using the Rneasy micro kit (Qiagen). For isolation of the PNVP/meninges, the brain was removed from the embryo and fine forceps were used to peel the PNVP/meninges layer from the telencephalic vesicles. RNA concentration was determined using UV spectrophotometer and 500ng of RNA was reverse-transcribed using the iScript cDNA synthesis kit (Bio-Rad) according to manufacturer's instructions. cDNA was amplified using real time RT-PCR with iScript One-Step RT-PCR kit with SYBR Green (Bio-Rad). A 12.5 μl reaction volume containing 6.25 μl of the SYBR Green PCR, 200nM of each primer was run, using the CFX Connect™ Real-Time PCR Detection System (Bio-Rad). The amplification program consisted of initial denaturation at 95°C for 3 minutes followed by 39 cycles of 95°C for 10 seconds and annealing at 60°C for 30 seconds. Primers used are as follows - VEGF-A: sense 5′-CAGGCTGCTGTAACGATGAA-3′ and antisense 5′-TTTGACCCTTTCCCTTTCCT-3. *Actb*: sense 5′-CTAGGCACCAGGGTGTGAT-3′ and antisense 5′-TGCCAGATCTTCTCCATGTC-3; *Dkk1*: sense 5′-GCCTCCGATCATCAGACTGT-3′ and antisense 5′- GCTGGCTTGATGGTGATCTT-3′; *Sfrp1* sense 5′- GAGTTTTGTTGCGGACCTGT -3′ and antisense 5′-GCCAGGGACAAAGCTAATGA -3′; *Sfrp2:* sense 5′-CTTGTGGGTCCCAGACTTA-3′ and antisense 5′-GCATCATGCAATGAGGAATG-3′; *Sfrp4:* sense 5′-ACCCTGGCAACATACCTGA -3′ and antisense 5′- CATCTTGATGGGGCAGGATA-3′; *Sfrp5*: sense 5′- GAGCCCAGAAGAAGAAGA -3′ and antisense 5′-TTCTTGTCCCAGCGGTAGAC -3′; *CDH5:* sense 5′-CAACTTCACCCTCATAAACAACC- 3′ and antisense 5′- ACTTGGCATGCTCCCGATT-3′; *ALDH1A2:* sense 5′- GACGCCGTCAGCAGGAAAA- 3′ and antisense 5′-CGCCAATCGGTACAACAGC -3′; *CSPG4:* sense 5′- GGGCTGTGCTGTCTGTTGA- 3′ and antisense 5′- TGATTCCCTTCAGGTAAGGCA- 3′; *Actb* gene was used as an internal control for normalization in all PCR reactions. Relative quantification of fold-change in mRNA expression was determined using the 2-DDCT method (Livak and Schmittgen, 2001). Fold change was calculated relative to cortical progenitor cells with no treatment (control) in the cell culture system and relative to *Foxc1* control genotypes *(Foxc1*$^{+/+}$ *and Foxc1*$^{lacZ/+}$*, Foxc1*$^{hith/+}$*)* with no RA dietary exposure..

ELISA analysis

Neocortices were isolated from E14.5 control and *Foxc1*$^{hith/lacZ}$ non-treated (n=3 for each genotype) and RA-treated embryos (n=3 for each genotype). Tissues were lysed in RIPA buffer (Sigma) containing a protease inhibitor cocktail tablet (Roche). Conditioned medium and cell lysates were collected from control (untreated), RA treated and RA+pan-RAR antagonist treated mouse E14 cortical progenitor cells or differentiated neurons, cultured for 24 hours in treatment conditions. For WNT7a and WNT7b, VEGF-A and VEGF-C protein

levels from tissue or cell lysates and conditioned medium were measured using ELISA kits (VEGF-A: R&D Systems and VEGF-C, WNT7a, WNT7b: Antibodies-Online) according to the manufacturer's instructions.

Statistics

To detect statistically significant differences in mean values between a control and mutant genotype at one developmental time point, Student *t*-tests were used. Analysis that compared more than two groups (e.g., two genotypes and two treatment conditions), a one-way analysis of variance (ANOVA) with Tukey's post-hoc analysis was used to detect statistically significant differences between genotypes or treatment conditions using pairwise analysis. The standard error of the mean (SEM) is reported on all graphs.

Results

Foxc1 hypomorph and knockout mice display vascular defects in the cerebral cortex prior to cerebral hemorrhage

Severe cerebral hemorrhage has been reported in a spontaneously occurring *Foxc1* mutant *Congenital hydrocephalus* (*Ch*) (Gruneberg, 1943) and an engineered *Foxc1-LacZ* knockout mouse ($Foxc1^{Lacz/Lacz}$) at E18.5 (Kume et al. 1998; Siegenthaler et al. 2009). This phenotype points to defects in formation of blood vessels within the cerebral cortex. We examined cerebrovascular morphology in *Foxc1* hypomorph mutants ($Foxc1^{hith/hith}$) that have a milder phenotype (Zarbalis et al. 2007; Siegenthaler et al. 2009) and *Foxc1-lacZ* global knockout mutants ($Foxc1^{lacZ/lacZ}$) at E14.5 and E16.5, time points when both the PVVP and PNVP-derived vessels are actively growing within the neocortex. To visualize the vasculature in the cortex, we performed immunofluorescence (IF) for glucose transporter-1 (GLUT1) on sections from wildtype (WT), $Foxc1^{hith/hith}$ and $Foxc1^{lacZ/lacZ}$ mutants. GLUT1 is enriched in the CNS vasculature and in red blood cells (RBCs). This allowed us to distinguish PNVP in the meninges from non-neural vasculature in the overlying mesenchyme and skin and to visualize RBCs in the neural parenchyma, suggestive of hemorrhage. In the cerebral wall at E14.5, GLUT1+ vessels were stunted and dilated in both types of *Foxc1* mutants compared to WT, though no hemorrhage was ever observed at this age (Fig. 1A-C). The PNVP adjacent to the cortex was thickened and contained enlarged vessels (arrows in Fig. 1B, C). Quantification of E14.5 cerebral vessel density (Fig. 1D) and diameter (Fig. 1E) revealed significantly lower vessel density but significantly enlarged vessels in both *Foxc1* mutant gentoypes ($p<0.05$; $n=4$). At E16.5, dilated vessels were frequently observed in the cortex of $Foxc1^{hith/hith}$ mutants (Fig. 1G). The dysplastic cortex of $Foxc1^{lacZ/lacZ}$, outlined by dashed lines, had disorganized, dilated vessels and hemorrhage (Fig. 1H; asterisks indicated GLUT1+ RBCs in the parenchyma). Though active hemorrhaging was less severe in the pictured $Foxc1^{lacZ/lacZ}$ mutant, about half of E16.5 and all E18.5 $Foxc1^{lacZ/lacZ}$ mutants display the widespread cerebral hemorrhage (Fig. 1I; arrowhead). In contrast, $Foxc1^{hith/hith}$ mutants did not display overt prenatal brain hemorrhage (Fig 1I) although at birth $Foxc1^{hith/hith}$ mutants often had a distinct bruise on the top of their heads (Fig. 1J; arrow). This was due to hemorrhage both within and around the cortex that presumably occurred during parturition (Fig. 1K; arrows). Possibly, the dorsal

calvarial defects in these *Foxc1*$^{hith/hith}$ mutants described previously (Zarbalis et al. 2007) leave the PNVP vasculature vulnerable to sheer-force induced damage during birth.

Foxc1 mutants have significantly enlarged cerebral hemispheres at E14.5 and these morphological defects could contribute to the impaired vasculature. To explore this further, we examined cerebrovascular morphology in *Foxc1* knockouts at E12.5 which is a time point when the cerebral expansion is visible milder in these mutants (Supp. Fig. 1A & B). To visualize the vasculature in the cortex, we performed IF for GLUT1 and isolectin b4 (Ib4) on sections from WT and *Foxc1*$^{lacZ/lacZ}$ mutants. In the cerebral wall at E12.5, GLUT1+ vessels were fewer and dilated in *Foxc1* mutants compared to WT (Supp. Fig.1B, C). The PNVP adjacent to the cortex was thickened and contained enlarged vessels. Quantification of E12.5 cerebral vessel density (Supp. Fig.1G) and PNVP and cerebral vessel diameter (Supp. Fig. 1E-F) revealed significantly lower vessel density but significantly larger vessel diameter in *Foxc1* mutants at E12.5. This is consistent with recent reports that defects in the Foxc1 mutant telencephalic vasculature appear as early as E10 in the ventral telencephalon (Prasitsak et al., 2015).

Foxc1 is expressed by brain pericytes and endothelial cells but deletion of Foxc1 in these cell types does not recapitulate the cerebrovascular defects of global *Foxc1* mutants.

To determine whether the cerebrovascular defects could be caused by loss of *Foxc1* expression in the brain vasculature, we used the β-galactosidase (β-gal) activity driven by the *Foxc1* promoter in *Foxc1*$^{lacZ/+}$ embryos and immunostaining for Foxc1 protein to determine when and where it is expressed in the brain vasculature. At E11.5, β-gal activity corresponding to *Foxc1* expression was strongest in the mesenchyme surrounding the CNS and the eye (Fig. 2A). Neural tissue was devoid of Foxc1 expression except for strings of β-gal+ cells in the forebrain (FB), midbrain (MB) and hindbrain (HB); this pattern is typical of blood vessels with associated perivascular cells, namely pericytes (Fig. 2A', A", and A"'). Immunostaining for Foxc1 and PDGFrβ (expressed by meningeal fibroblasts and pericytes) showed Foxc1+ nuclei in the meninges and PNVP overlaying the neocortex (Fig. 2B). A higher magnification image in the neocortex depicts Foxc1+/Pdgfrβ+ pericytes (PC) and Foxc1+ endothelial cell (EC) nuclei in the vessel lumen (Fig. 2B'). We further confirmed Foxc1 expression in pericytes and endothelial cells by co-labeling with endothelial marker IB4. As shown in Fig. 2C, Foxc1+ endothelial nuclei were visible within the IB4+ vessel where Foxc1+ pericyte nuclei, which did no co-label with IB4, were seen on the vessel surface.

To evaluate the requirement for Foxc1 in endothelial cells, we used *Tie2-Cre* to conditionally ablate *Foxc1* from endothelial cells (*Tie2-Cre; Foxc1-fl/fl*). This resulted in viable, adult mutants with no obvious alteration in cerebral vasculature relative to control littermates (*Tie2-Cre; Foxc1-fl/+*), as shown labeled with endothelial cell marker PECAM and pericyte marker desmin (Fig. 2D & E). This data suggests that Foxc1 expression in endothelial cells may be dispensable for brain vascular development and maintenance however it is possible that Foxc2, a close homolog of Foxc1, may be upregulated in *Tie2-Cre; Foxc1-fl/fl* mutants and can compensate for loss of Foxc1. Foxc2 is expressed in a

subset of meningeal cells however it is not detected in the E14.5 brain vasculature (Siegenthaler et al., 2013).

We have shown previously that conditional deletion of *Foxc1* from pericytes using the *Pdgfrβ-Cre* line does not result in severe cerebrovascular defects (Siegenthaler et al., 2013). We do consistently observe dilated cerebral vessels in the E16.5 *Pdgfrb-Cre; Foxc1-fl/fl* mutant (Fig. 2F) although we have shown previously that, unlike global *Foxc1* mutants, vascular growth is not diminished in conditional mutants (Siegenthaler et al., 2013).

We also examined neurovascular development in a different forebrain structure, the thalamus, of global *Foxc1* knockout mice. Our reasoning for this is if Foxc1 controls brain vascular growth via its expression in endothelial cells and/or pericytes we would expect vascular defects to be present in all brain regions. In contrast to the reduction in cerebrovascular density in E14.5 $Foxc1^{lacZ/lacZ}$ neocortex (Fig. 2H, I), GLUT1+ blood vessels in the $Foxc1^{lacZ/lacZ}$ thalamus were indistinguishable from littermate controls (Fig. 2J, K). We quantified thalamic blood vessel diameter in E14.5 control and $Foxc1^{lacz/lacz}$ mutants and found no significant difference in mean thalamic blood vessel diameter (control: 11 μm ± 0.625 vs $Foxc1^{lacZ/lacZ}$: 10.751 μm ± 0.328; n=3). This contrasts with E14.5 $Foxc1^{lacZ/lacZ}$ neocortices in which blood vessel diameter is significantly increased (Fig. 1E). This analysis is consistent with a recent report showing that, in contrast to the telencephalon, vascular density in the hindbrain was unchanged in global *Foxc1* knockout mice (Prasitsak et al., 2015). Taken together, this data shows that conditional deletion of *Foxc1* from endothelial cells or pericytes does not recapitulate the severe cerebrovascular defects observed in global *Foxc1* mutants.

Wnt1-Cre; Foxc1-fl/fl mutants have neocortical and cerebrovascular defects closely resembling global *Foxc1* mutants

Foxc1 is expressed by meningeal fibroblasts and *Foxc1* mutants have defects in formation of the meninges overlying the neocortex (Siegenthaler et al., 2009). Thus we next tested if Foxc1 functions in meningeal fibroblasts to regulate cerebrovascular development. To do this we used *Wnt1-Cre*, previously shown to recombine in neural crest lineages but not mesoderm which gives rise to endothelial cells, to conditionally delete Foxc1 during development. We confirmed reports that *Wnt1-Cre* recombines telencephalic meninges using the *Rosa26-YFP* Cre reporter line (Jiang et al., 2002). The meningeal layer adjacent to the telencephalon showed robust recombination, as detected by immunolabeling with an anti-GFP antibody that cross-reacts with YFP (Fig. 3B, B'). We also observed recombination in pericytes that were surrounding PECAM+ blood vessels (Fig. 3A, B). This was expected as telencephalic pericytes are neural crest-derived (Etchevers et al., 2001). Importantly, we did not observe recombination in mesoderm-derived PECAM+ endothelial cells (Fig. 3B, B'). We examined E14.5 *Wnt1-Cre; Foxc1-flox* control and mutant animals and compared them to global *Foxc1* knockouts ($Foxc1^{lacZ/lacZ}$). Tuj1 immunostaining to label young neurons highlighted the strikingly similar defects in telencephalic development, namely elongation of the neocortex, in *Wnt1-Cre;Foxc1-fl/fl* and $Foxc1^{lacZ/lacZ}$ mutants (Fig. 3D, E). Furthermore, cerebral cortices of *Wnt1-Cre;Foxc1-fl/fl* mice showed blood vessel defects comparable to those seen in $Foxc1^{lacZ/lacZ}$ as observed by PECAM to label blood vessels

(Fig. 3G, H). Conditional deletion of *Foxc1* from the *Wnt1-Cre* recombined cells, which includes telencephalic meninges and brain pericytes, appears to recapitulate the cerebrovascular defects observed in global *Foxc1* mutants. Furthermore, this points to Foxc1 expression in the meninges as having an important function in cerebrovascular development.

Exposure to exogenous RA improves cerebrovascular development in *Foxc1* mutants

Secreted signals from the telencephalic meninges are required for neocortical development and one of the important signals made by the meninges is RA. The RA-synthesizing layer of the meninges overlyaing the neocortex does not form completely in *Foxc1* mutants and thus reduces the amount of RA in the neocortex and the PNVP/meningeal space (Siegenthaler et al., 2009). We tested whether exposing *Foxc1* mutants to exogenous *all-trans* RA (atRA) via maternal diet from E10.5 to E14.5, a treatment we previously showed improves neocortical development (Siegenthaler et al., 2009), can restore normal development of the cerebrovasculature (Fig. 4A). For these experiments, we used $Foxc1^{hith/lacZ}$ mutant mice as they have more severe defects in corticogenesis than $Foxc1^{hith/htih}$ mutants and maternal RA treatment effectively rescues their defects in neocortical development (Siegenthaler et al. 2009). We performed IF for GLUT1 on E14.5 brain sections of control ($Foxc1^{+/+}$, $Foxc1^{hith/+}$ or $Foxc1^{lacZ/+}$) and $Foxc1^{hith/lacZ}$ mutants collected from dams fed a normal or RA-enriched diet. We analyzed three parameters of vascular growth within the cerebral wall: 1) vessel branch point frequency, 2) number of blood vessels entering the cerebral wall from the overlaying PNVP and 3) blood vessel diameter. Whole embryo images (Fig. 4B) and low-magnification images at the level of the forebrain of control and $Foxc1^{hith/lacZ}$ mutants (Fig. 4C-F) on normal and RA-enriched diet highlights the improvement in cerebral hemisphere size in $Foxc1^{hith/lacZ}$ mutants with RA exposure (Fig. 4B; compare 4D and 4F). In non-RA treated $Foxc1^{hith/lacZ}$ embryos, branching of vessels within the neocortex was notably reduced, vessels had larger diameters and very few PNVP-derived vessels were observed as compared to non-RA treated control (Fig. 4G, H). Quantification revealed a significant decrease in the number of cerebral vessel branch points and number of PNVP-derived vessels as well as an increase in vessel diameter (Fig. 4K, L, & M; $p<0.05$ n=3). In RA-exposed control animals, there was no significant change in branch point density or diameter as compared to non-RA treated control embryos (Fig. 4K & M) however there was a significant decrease in the number of PNVP-derived vessels (Fig. 4L; $p<0.05$ n=3). This indicates that excess RA has a specific effect on growth of vessels from the PNVP into the cerebral wall. Most compelling was the effect of RA on cerebrovascular development in $Foxc1^{hith/lacZ}$ mutants (compare Fig. 4H & J). Branch point density (Fig. 3K) and number of PNVP-derived vessels (Fig. 3L) was significantly greater than non-RA treated $Foxc1^{hith/lacz}$ mutants and vessel diameter was not significantly different from control (Fig. 3M; n=3).

During angiogenesis, endothelial cells that make up blood vessels proliferate and undergo angiogenic sprouting, forming vessel branches and eventually an intricate blood vessel network (Vallon et al., 2014). The decrease in the number of vessel branch points could be caused by decreased endothelial cell proliferation. To measure this, the thymidine analog bromodeoxyurdine (BrdU) was injected into pregnant dams and embryos were collected 2 hours later and we used endothelial transcription factor ERG1 to label endothelial cell nuclei (Arnold et al., 2014). We quantified the percentage of ERG1+ endothelial cells in S-phase as

indicated by co-immunolabeling for BrdU. In *Foxc1*$^{hith/lacz}$ mutants, the percentage of ERG1+ endothelial cells co-labeled with BrdU+ was significantly reduced as compared to control (Fig. 4N, O & R; $p<0.05$ n=4). In contrast, endothelial cell proliferation was not significantly different from control in RA-exposed *Foxc1*$^{hith/lacz}$ mutants (Fig. 3P, Q, & R; n=4). Proliferating ECs are usually found in an angiogenic sprout, generally in the 'stalk cell' position adjacent to the filopodia rich tip cell. To complement our proliferation analysis, we examined the percentage of cerebral vessels with tip cell characteristics, namely filopodia. GLUT-1 IF highlighted numerous tip cells with filapodia in the cerebral vasculature of non-RA and RA-exposed control embryos however notably fewer filapodia containing tip cells were evident in *Foxc1*$^{hith/lacZ}$ mutants (Supp. Fig. 2A-C). RA exposure notably increased the incidence of filopodia-containing tip cells in *Foxc1*$^{hith/lacZ}$ mutants. Quantification revealed a significant decrease in the percentage of cerebral vessels with filopodia in *Foxc1*$^{hith/lacZ}$ mutants as compared to untreated control (Supp. Fig. 2E, $p<0.05$ n=3). In RA-exposed control animals, there was no significant change compared to non-RA treated control embryos (Supp. Fig. 2E $p<0.05$ n=3) however, the decrease in percentage of cerebral vessels with filopodia was rescued with atRA diet as evidenced by significant increase in filopodia in atRA treated *Foxc1*$^{hith/lacZ}$ mutants as compared to untreated *Foxc1*$^{hith/lacZ}$ mutants (Supp. Fig. 2E; $p<0.05$ n=3).

Taken together, our observation that defects in cerebrovascular growth and endothelial cell proliferation can be rescued with maternal fed RA suggests that loss of meningeal-derived RA contributes to the cerebrovascular defects in *Foxc1* mutants.

Endothelial cell specific disruption of RA signaling does not recapitulate *Foxc1* mutant cerebrovascular defects

The cerebrovascular defects in *Foxc1* mutants could be due to reduced RA signaling in neocortical endothelial cells caused by loss of meningeal-derived RA. If this is the case we would expect that specifically disrupting RA signaling in endothelial cells would cause similar cerebrovascular defects as seen in *Foxc1* mutant neocortices. To test this idea we used an inducible, endothelial cell specific Cre line (*Pdgfbi-Cre*) to express a dominant negative retinoic acid receptor (*dnRAR403-flox*), previously shown to disrupt RA signaling when expressed in a cell (Rosselot et al., 2010), in endothelial cells during neocortical development. This truncation mutant of human RARα has been shown previously to block RAR-mediated signaling through all three RAR isoforms (Damm et al., 1993; Tsai et al., 1992). We analyzed the same three parameters of vascular growth as we did with *Foxc1* mutants within the cerebral wall of E14.5 control (wildtype or *dnRAR403 fl/fl*) or endothelial RA signaling mutants (*Pdgfbi-Cre; dnRAR403-fl/fl*): 1) vessel branch point frequency, 2) number of blood vessels entering the cerebral wall from the overlaying PNVP and 3) blood vessel diameter. Low-magnification images of sections immunostained with GLUT-1 and vascular label isolectin-B4 (IB4) show that, unlike *Foxc1* mutants, the forebrain structure and its vasculature was not overtly different between control and mutants (Fig. 5A, B; n=3). High magnification images of the E14.5 cerebrovasculature co-labeled with GLUT-1 and IB4 showed comparable branchpoint density and diameter (Fig. 5C, D) and quantification revealed no significant difference in these parameters (Fig. 5E, G; n=3). There appeared to be reduced number of blood vessels entering the cerebral wall from the

overlying PNVP in endothelial RA signaling mutants however the difference was not statistically significant (Fig. 5C, D, & F; n=3). Interestingly, analysis of endothelial cell proliferation showed a significant increase in labeling index in RA signaling mutants at E14.5 (Fig. 5H, I & J; $p<0.05$ n=3). These data show that endothelial RA signaling is likely important for cerebrovascular development however the phenotype is different than *Foxc1* mutants, indicating that the cerebrovascular defects in *Foxc1* mutants are unlikely to be entirely due to a disruption in endothelial RA signaling.

Reduced number of PNVP-derived vessels in *Foxc1* mutants correlates with decreased endothelial WNT signaling in the PNVP

Endothelial WNT signaling is required for neurovascular growth and stability (Stenman et al. 2008; Daneman et al. 2009). Thus we investigated whether endothelial WNT signaling was disrupted in the cerebrovasculature of E14.5 *Foxc1* mutants. To do this we used a WNT signaling transgenic mouse line, *Bat-gal-lacZ* in which expression of β-galactosidase (β-gal) is a read-out of recent WNT transcriptional activity within a cell. We examined β-gal expression in endothelial cells (as determined by co-localization with blood vessel marker IB4+) in the PNVP (Fig. 6A-D). β-gal+ endothelial cells were apparent in the PNVP layer adjacent to the neocortex in control animals however there were significantly fewer β-gal+ endothelial cells in $Foxc1^{hith/lacZ}$ mutant PNVP layer (Fig. 6A, B and E; $p<0.05$ n=3). Interestingly, there was also a significant decrease in β-gal+ endothelial cells within the PNVP of control animals exposed to RA (Fig. 6C and E; $p<0.05$ n=3). In $Foxc1^{hith/Lacz}$ mutants exposed to RA prenatally, the number of β-gal+ endothelial cells within the PNVP was significantly elevated as compared to non-RA treated control and $Foxc1^{hith/Lacz}$ mutants (Fig. 6D and E; $p<0.05$ n=3).

To test if loss of endothelial Wnt signaling can result in reduced growth of vessels into the cerebral wall from the PNVP, we examined another mouse model system wherein β-catenin, a major component of Wnt signaling pathway, is conditionally deleted in endothelial cells. We used the endothelial cell specific *Pdgfbi-Cre* (Claxton et al. 2008) with the conditional β-catenin null allele (*Ctnnb1-flox*) which allowed us to delete β-catenin from endothelial cells at ~E12, a time point when the ventral to dorsal growth of the PVVP within cerebral wall is complete but prior to the appearance of PNVP-derived vessels growing into cerebral wall (Fig. 6F). In E14.5 *Pdgfbi-Cre; Ctnnb1-fl/fl* mutants, the PVVP within the cerebral wall was present but notably less complex than the control littermate (Fig. 6G, H). Similar to *Foxc1* mutants, there were significantly fewer PNVP-connected vessels in *Pdgfbi-Cre; Ctnnb1-fl/fl* (Fig. 6I; $p<0.05$ n=3). This data supports the idea that failure of vessels to grow from the PNVP into the $Foxc1^{hith/lacZ}$ mutant neocortex is caused by reduced endothelial Wnt signaling in the PNVP.

WNT inhibitors are increased in *Foxc1* mutant PNVP/meninges and this is rescued with exogenous RA treatment

We next tested if reduced endothelial WNT signaling in the PNVP of *Foxc1* mutants and diminished blood vessel growth into the cortex could be a result of altered expression of WNT signaling inhibitors Dkk1 and soluble frizzled receptor proteins (SFRPs) in the PNVP/meninges. This idea is based on data that RA suppresses Dkk1 in the developing foregut

(Chen et al., 2010) and our own work showing that RA-deficient mutants (*Rdh10* hypomorphs) have elevated soluble WNT inhibitors in the neocortex (Bonney et al., 2016). We used real-time PCR to compare gene expression of WNT inhibitors *Dkk1, Sfrp1, Sfrp2, Sfrp4* and *Sfrp5* in PNVP/meninges tissue isolated from the telencephalon of control and *Foxc1* mutants ± RA exposure. The isolated PNVP/meningeal tissue was comprised of a mixed population of cell types as determined by qPCR, which showed gene expression of *Aldh1a2* (Raldh2), *Cspg4* (Ng2) and *Cdh5* (VE-Cadherin) representing meningeal fibroblasts, pericytes and endothelial cells, respectively (Supp. Fig. 3). *Cspg4* gene expression was increased in *Foxc1* mutants likely due to increased pericyte numbers and *Aldh1a2* expression was significantly decreased due to reduced meningeal cells, two phenotypes we have previously described in these mutants (Siegenthaler et al., 2009; Siegenthaler et al., 2013). We detected a moderate to substantial increase in the transcript expression of *Dkk1* and *Sfrps* in PNVP/meninges tissue from *Foxc1* mutants relative to control and these increases were rescued by treatment with RA (Fig. 6J; $p<0.05$ n=3). This result indicates meningeal-derived RA may normally suppress WNT inhibitor expression in the meninges/PNVP but this does not occur in *Foxc1* mutants that lack RA-synthesizing meninges.

Taken together, our data indicates that WNT signaling is specifically affected in the neocortical PNVP and, possibly, contributes to the failure of PNVP vessels to grow into superficial portions of the $Foxc1^{hith/Lacz}$ cerebral wall. Furthermore, the rescue of the phenotype by exogenous RA suggests a specific role for meningeal derived-RA in control of PNVP Wnt signaling.

Vessels within *Foxc1* mutant neocortices have normal endothelial Wnt signaling though Wnt7a/b ligand expression is reduced

To test if endothelial WNT signaling is also disrupted in the neocortical vasculature of *Foxc1* mutants, which consists mostly of the PVVP, we used the *Bat-gal-lacZ* transgenic mouse line to examine endothelial WNT activity (Fig. 7A-D). Blood vessels within the cerebral wall did not have a significant difference in the number of β-gal+ endothelial cells between control and $Foxc1^{hith/Lacz}$ mutants and neither genotype was affected by prenatal RA exposure (Fig. 7 A, D; # Bat-gal+ ECs/# cerebral blood vessels per field - control: 0.52 ± 0.053; $Foxc1^{hith/Lacz}$: 0.5 ± 0.14; control+RA: 0.49 ± 0.005; $Foxc1^{hith/Lacz}$ + RA: 0.67 ± 0.06 p=0.558 n=3). This suggests that alterations in endothelial WNT are likely not a major contributor factor to the defects in *Foxc1* mutant PVVP.

WNT signaling in CNS endothelial cells, including those in the PNVP, is stimulated by WNT ligands WNT7a and WNT7b that are expressed by neuronal progenitors in the VZ as well as post-mitotic neurons (Stenman et al. 2008; Daneman et al. 2009). Deletion of WNT7a and WNT7b severely impairs growth of vessels into the brain and spinal cord (Stenman et al.2008; Daneman et al.2009). The reduction in WNT signaling in the PNVP layer and subsequent rescue by prenatal RA exposure suggests that neural WNT7a and WNT7b expression may be affected by loss of meningeal-derived RA. To test this, we first used *in situ* hybridization to evaluate *Wnt7a* and *Wnt7b* transcript expression in the neocortex at E14.5 in non-RA and RA treated *Foxc1* mutant embryos. Within the cerebral

wall, *Wnt7a* signal was highest in the VZ and in neurons within the superficial portion of the cortical plate adjacent to the PNVP (Fig. 7E). In the *Foxc1*$^{hith/lacZ}$ mutant cerebral wall the *Wnt7a* signal, qualitatively, appeared less intense and the width of the *Wnt7a* expressing zone within the *Foxc1*$^{hith/lacZ}$ cortical plate was much thinner (Fig. 7F). In RA-exposed *Foxc1*$^{hith/lacZ}$ mutant cerebral wall, however, the *Wnt7a*-labeled cortical plate and VZ was comparable in size to the control and the intensity of the signal appeared elevated (Fig. 7G). *Wnt7b* transcript was not observed in the VZ and the intensity was highest in post-mitotic neurons within the cortical plate (Fig. 7H). The cortical plate was thinner in *Foxc1*$^{hith/lacz}$ mutants, owing to defects in neuron generation (Siegenthaler et al. 2009). Thus the *Wnt7b* expressing *Foxc1*$^{hith/lacz}$ cortical plate was reduced in thickness and this was rescued with exposure to RA (Fig. 7I, J). This analysis of *Wnt7a* and *Wnt7b* expression suggests *Foxc1* mutant may have lower expression of these ligands due to a reduced number of *Wnt7a* and *Wnt7b*-producing cells in the cerebral wall, notably the cortical plate, and possibly less expression on a per cell basis. We quantified via ELISA WNT7a and WNT7a ligand protein levels in neocortical lysates from E14.5 control and *Foxc1*$^{hith/lacz}$ mutants ± RA exposure (Fig.7K). RA-exposure in control embryos significant increased WNT7a and WNT7b protein expression (Fig. 7K; $p<0.05$ n=3). WNT7a and WNT7b ligand protein levels were significantly reduced in *Foxc1*$^{hith/lacz}$ mutant neocortices relative to control, non-RA treated lysates but WNT ligand levels were rescued to control levels in RA-exposed *Foxc1*$^{hith/lacz}$ mutant (Fig.7K; $p<0.05$ n=3). This data indicates that RA may directly stimulate WNT7a and WNT7b expression in neocortical progenitors and/or neurons. In support of this, we found atRA treatment of primary neocortical progenitors derived from embryonic mouse neocortex increased WNT7a and WNT7b protein in the cell lysate, an effect that was inhibited by a pan-RAR inhibitor (Fig 7L; $p<0.05$ n=3). However, atRA treatment of primary cortical neurons had no effect WNT ligand levels (Fig 7M; n=3). This data suggests that RA may specifically act upon progenitors to stimulate WNT ligand expression or cortical neurons in culture have a different response to RA than *in vivo*.

Reduced VEGF-A protein expression in *Foxc1* mutant neocortices is rescued by RA treatment

Our observation that endothelial WNT signaling was not significantly altered within the *Foxc1* mutant neocortex, yet we observe significant defects in branching, endothelial cell proliferation and tip cells within the neocortex suggests there is a different angiogenic pathway that underlies these defects in vascular growth. VEGF-A is a potent, pro-vascular growth factor expressed by neocortical progenitors in the VZ and conditional deletion of VEGF-A in neural progenitor cells leads to severe defects in vascular growth into the brain and spinal cord (Breier et al., 1992; Darland et al., 2011; Haigh et al., 2003; James et al., 2009; Raab et al., 2004). Therefore we sought to determine whether VEGF-A was affected in *Foxc1* mutants. We quantified VEGF-A protein concentrations in E14.5 neocortices using an ELISA and found that VEGF-A protein levels were significantly reduced in *Foxc1*$^{hith/lacZ}$ mutants relative to littermate control cortices (Fig. 8A; $p<0.05$ n=6). RA treatment produced two interesting findings with regard to VEGF-A. First, RA-exposure significantly increased VEGF-A protein concentrations in control neocortices (Fig. 8A; $p<0.05$ n=3). Second, VEGF-A protein levels in *Foxc1*$^{hith/lacZ}$ mutant neocortices exposed to RA were significantly higher than non-RA treated controls and *Foxc1*$^{hith/lacz}$ mutants (Fig.8A). This

data demonstrates that *Foxc1* mutants have reduced VEGF-A levels in the neocortex and this may be caused by loss of RA from the meninges. To see if the effect of RA was specific for VEGF-A, we examine expression of another VEGF ligand produced by neural cells during development, VEGF-C (Le Bras et al., 2006; Ward and Cunningham, 2015). In contrast to VEGF-A, VEGF-C protein levels quantified by ELISA were not significantly different in *Foxc1* mutant neocortices and were unaffected by RA exposure (Fig. 8B; n=3).

RA stimulates VEGF-A expression in neocortical progenitor cultures

VEGF-A is specifically expressed by neocortical progenitors in the VZ of the developing neocortex (Breier et al., 1992; Yang et al., 2013). To test if loss of VEGF-A in *Foxc1*$^{hith/lacZ}$ mutant neocortices is a result of direct effect of RA on cortical progenitors, we utilized neocortical progenitor cells derived from E14.5 mouse neocortices. Culturing cells in hypoxia (3% O_2), a known stimulant of VEGF-A expression, significantly increased *Vegfa* gene expression as did treatment with 1 μM atRA (Fig. 8C; $p<0.05$ n=3). The effect of RA in *Vegfa* expression was blocked when cells were co-treated with atRA and a pan-RAR antagonist (Fig. 8C). VEGF-A ELISA of conditioned media from control and atRA-treated cortical progenitor cells showed progenitors treated with RA increased VEGF-A protein release into culture medium as compared to control (Fig. 8D; $p<0.05$ n=3). The effect of RA on VEGF-A in the medium was inhibited in progenitors co-treated with atRA and pan-RAR antagonist (Fig. 8D). These results demonstrate that RA can stimulate VEGF-A release from cortical progenitor cells. Further, it supports our model that loss of meningeal-derived RA in *Foxc1* mutants decreases VEGF-A expression and contributes to the diminished cerebrovascular growth in these mutants.

Discussion

Cerebrovascular development requires growth of blood vessels from two plexuses, the PVVP and PNVP, and is driven by angiogenic ligands derived neural cells in the rapidly developing cerebral wall. Here we demonstrate that the transcription factor Foxc1 plays an important role in cerebrovascular development via regulating formation of the meninges, an important source of signals like RA for the developing neocortex. Importantly, our observations demonstrate meningeal-derived RA plays a previously unrecognized role in regulating WNT and VEGFA pathways, both required for cerebrovascular growth. This work not only brings to light an interaction between the meninges and the brain vasculature it provides important insight into the molecular mechanism underlying cerebrovascular defects in patients with mutations or deletions in *FOXC1.*

We show that vascular growth defects precede severe cerebral hemorrhage by several days, a finding consistent with published analysis of ventral vascular defects in an early *Foxc1* mutant telencephalon (Prasitsak et al., 2015). Our observations bring up two important considerations. First, what is the significance of early defects in ventral telencephalic vascular development in *Foxc1* mutants to the later growth defects we observe in the neocortex? Telencephalic vascular development occurs differently than in other brain regions: the PVVP first appears in the VZ of the ventral telencephalon at ~E10 then grows dorsally into the neocortical VZ between E11 and E12 (Vasudevan et al., 2008). Early

defects in the formation of the ventral PVVP could delay growth into the neocortex and contribute to some of the later cerebrovascular defects. However, it is unlikely the primary cause since we show endothelial cell proliferation is decreased at E14.5 and growth from a separate vascular plexus, the PNVP, is also diminished in *Foxc1* mutant neocortices. Second, how do the cerebrovascular defects we observe at E14.5 lead to the widespread vascular instability and cerebral hemorrhage at later stages? We find increased blood vessel diameter in the *Foxc1* mutant cerebrovasculature and it is possible this diameter increase is due to vascular wall shear stress (Silber et al., 2001). Arterial blood flow pressure in an underdeveloped vascular plexus possibly creates undue stress on already dysplastic vessels and causes them to rupture. Additionally, mice lacking pericytes show endothelial cell hyperplasia and defective capillary morphogenesis (Hellstrom et al 2001). *Foxc1* is expressed by pericytes and conditional deletion of *Foxc1* from pericytes leads to dysplastic vessels and late gestation cerebral micro-hemorrhages (Siegenthaler et al. 2013). Thus, pericyte dysfunction caused by loss of Foxc1 almost certainly contributes to the cerebral hemorrhage observed in global *Foxc1* mutants.

Our analysis of global *Foxc1* mutants provides important insight into the development and mechanisms governing growth of vessels from the PNVP into superficial portions of the neocortex. Studies suggest growth of PNVP vessels into the neocortex is a separate event from development of the PVVP in the neocortical VZ (Strong, 1964; Vasudevan et al., 2008) and there is evidence that these two plexuses are molecularly distinct, as shown by differential gene expression (Won et al., 2013). We show that fewer PNVP vessels grow into the *Foxc1* mutant neocortex and to our knowledge this is the first description of a specific defect in the growth of this plexus in the neocortex. Further, we show that PNVP growth defects correlate with diminished endothelial WNT signaling in the PNVP. Endothelial WNT signaling is required for growth and maturation of vessels in the CNS (Daneman et al., 2009; Stenman et al., 2008; Zhou et al., 2014) thus our data points to loss of endothelial WNT signaling as a major factor contributing to this vascular phenotype. This is further supported by our observation that deletion of WNT signaling protein β-catenin from endothelial cells diminishes growth of PNVP vessels into the brain. Though we observe a correlation between loss of endothelial WNT and diminished growth of PNVP vessels into the neocortex, it is possible that other angiogenic pathways like Notch, TGFβ and VEGF are disrupted in the *Foxc1* mutant PNVP and contribute to the phenotype. Future work will address this possibility and determine if these possibly occur downstream of RA.

The reduction in endothelial WNT signaling in the *Foxc1* mutant PNVP appears to be due to loss of RA from the meninges since RA supplementation during development reverses the phenotype. How is RA from the meninges controlling PNVP endothelial WNT signaling? Based on our analysis we hypothesize this is caused by a combination of increased WNT inhibitor expression in the *Foxc1* mutant meninges/PNVP and decreased WNT ligands coming from the neocortex (Fig. 9). With regard to the former, RA has been shown to directly suppress *Dkk1* expression in the foregut as a means to increase WNT signaling (Chen et al., 2010). Possibly, RA synthesized by a subset of meningeal fibroblasts acts on mural cells or endothelial cells of the PNVP or meningeal fibroblasts to actively suppress expression of Dkk1 and SFRPs in the PNVP space. $Foxc1^{hith/lacZ}$ mutants used here lack most RA-synthesizing meningeal fibroblasts overlying the neocortex (Siegenthaler et al.,

2009), thus cells of the PNVP and remaining meningeal fibroblasts in the pial layer (included in the PNVP dissections) are exposed to much less RA locally. As a result, individual or multiple cell types upregulate expression of WNT inhibitors. Exposure to exogenous RA is sufficient to restore WNT inhibitor expression in the *Foxc1* mutant PNVP/meninges tissue. We believe this is a direct effect of RA on the PNVP or residual meningeal cells since RA treatment does not rescue defects in meningeal formation (Siegenthaler et al., 2009). Further studies are needed to determine which cells types express WNT inhibitors in the *Foxc1* mutants.

Our data on RA and neocortical WNT7 and WNT7b expression suggest two points of control for RA: 1) RA from the meninges regulates the generation of WNT ligand-producing cortical neurons and 2) RA directly stimulates expression of WNT ligands in neocortical progenitors and neurons. The latter point is supported by our data that RA exposure increases WNT7a and WNT7b in control neocortices *in vivo* and in cultured neocortical progenitors. Intriguingly, we do not observe a decrease in endothelial WNT signaling in blood vessels within the *Foxc1* mutant neocortex despite diminished levels of WNT7a and WNT7b ligands. It is important to note that the decrease in ligand expression, though statistically significant, is modest and our analysis indicates sufficient WNT ligands are produced to stimulate endothelial WNT signaling within the *Foxc1* mutant neocortex. Possibly, PNVP endothelial cells are more sensitive to even small reductions because they are separated from the neocortex by the ECM-rich pial basement membrane (Halfter et al., 2002). As a result, significant amounts of WNT ligands may be needed to stimulate PNVP endothelial cells. Though WNT ligands act as morphogens, they are not readily diffusible owing to post-translational modifications that make WNTs hydrophobic and interactions with glycosaminoglycan-modified proteins like heparin sulfate proteoglycan driving accumulation in the ECM (Mikels and Nusse, 2006).

An intriguing observation was that RA treatment significantly decreased endothelial WNT signaling in control PNVP and this was accompanied by decreased growth of vessels from the PNVP into the neocortex in RA-treated control animals. This finding is surprising given that RA treatment increases WNT7a and WNT7b ligand expression in control neocortices. However, RA is an established inhibitor of WNT signaling in other cell types through interaction of RA receptors with WNT signaling protein β-catenin (Chanda et al., 2013; Easwaran et al., 1999; Mulholland et al., 2005). Even more convincingly, we recently showed that the same RA signaling mutants used in these studies, *Pdgfbi-Cre; dnRAR403-fl/fl,* have elevated endothelial WNT signaling at a later developmental time point (Bonney et al., 2016). This, along with our observations about RA treatment on WNT signaling in the PNVP, suggests that RA is a direct inhibitor of endothelial WNT signaling. Here we show that E14.5 *Pdgfbi-Cre; dnRAR403-fl/fl* mutants do not have the severe cerebrovascular growth defects observed in *Foxc1* mutants but that there is phenotype, namely a significant increase in endothelial cell proliferation. We have found older *Pdgfbi-Cre; dnRAR403-fl/fl* mutant embryos have enlarged blood vessels and develop small microbleeds (Bonney et al., 2016). Thus, RA acting as an inhibitor of endothelial WNT signaling, plays in important role in vascular morphogenesis. It is possible that the vascular defects in *Foxc1* mutants could partially stem from reduced RA signaling in PNVP or neocortical vasculature. However, our results with regard to WNT pathway proteins and VEGF-A indicate that the cerebrovascular

defects are more likely due to reduced RA signaling in other cell types like VZ progenitors that make VEGF-A.

Our data points to loss of endothelial WNT signaling as a major underlying cause of defects in the PNVP development yet endothelial WNT signaling appears unchanged in vessels within the *Foxc1* mutant neocortex. Possibly, that the reporter line is not sensitive enough to detect subtle changes in endothelial WNT signaling. More likely, reduced VEGF-A expression by the *Foxc1* mutant neocortical VZ and, possibly, disruptions in other angiogenic pathways underlies the defects in growth and endothelial cell proliferation observed in the vascular plexus within the neocortex, which in *Foxc1* mutants consists almost entirely of the PVVP. VEGF-A is a well-established mitogen and promotes angiogenic sprouting in the CNS (Mackenzie and Ruhrberg, 2012), two cellular events that are diminished in the *Foxc1* mutant neocortex. While we believe that reduced VEGF-A expression results in defects in vascular growth in the *Foxc1* mutants PVVP, it is also possible that low VEGF-A levels, along with reduced WNT signaling, contribute to the failure of PNVP-derived vessels to grow into the neocortex.

We find that growth of the PVVP as well as VEGF-A protein expression was restored in *Foxc1* mutants with exogenous RA. Furthermore, we show that RA can directly stimulate VEGF-A expression in cultured neocortical progenitors. These data support a hypothetical model in which meningeal-derived RA regulates VEGF-A expression by VZ progenitors and in turn is required for PVVP development (Fig. 9). RA has been shown to upregulate expression of VEGF-A in several cell culture model systems (Liang et al., 2013, 2014; Wu et al., 2011). RA stimulates signaling in target cells through its receptors, RAR and RXR, which bind to DNA motifs known as retinoic acid response elements (RARE), in the promoter of the target genes (Ruberte et al., 1993). However, *Vegfa* promoter does not have a RARE sequence and thus RA may not act directly to regulate *Vegfa* transcription (Liang et al. 2013). HIF1A is the most potent transcriptional regulator of VEGFA (Pagès and Pouysségur, 2005) and RA has been shown to up regulate HIF1A in several cell types (Fernández-Martínez et al., 2012; Fernández-Martínez et al., 2011; Liang et al., 2014) Also, RARE sequences have been identified in the HIF1A promoter (Fernandez-Martinez et al. 2012). Future work will address the exact mechanism through which meningeal-derived RA regulates VEGF-A in the developing cerebral cortex.

Supplementary Material

Refer to Web version on PubMed Central for supplementary material.

Acknowledgments

This work was supported by the following funding agencies: National Institutes of Health/National Institute of Neurological Disorders and Stroke [K99-R00 NS070920 to J.A.S.], American Health Association/American Academy of Neurology [Lawrence M. Brass, M.D. Stroke Research Postdoctoral Fellowship to J.A.S.] and National Institutes of Health/National Institute on Drug Abuse [R01 DA017627 to S.J.P.].

References

Aldinger K, Lehmann O, Hudgins L, Chizhikov V, Bassuk A, Ades L, Krantz I, Dobyns W, Millen K. FOXC1 is required for normal cerebellar development and is a major contributor to chromosome 6p25.3 Dandy-Walker malformation. Nat Genet. 2009; 41:1037–1042. [PubMed: 19668217]

Armulik A, Genove G, Mae M, Nisancioglu MH, Wallgard E, Niaudet C, He L, Norlin J, Lindblom P, Strittmatter K, Johansson BR, Betsholtz C. Pericytes regulate the blood-brain barrier. Nature. 2010; 468:557–561. [PubMed: 20944627]

Arnold TD, Niaudet C, Pang MF, Siegenthaler J, Gaengel K, Jung B, Ferrero GM, Mukouyama YS, Fuxe J, Akhurst R, Betsholtz C, Sheppard D, Reichardt LF. Excessive vascular sprouting underlies cerebral hemorrhage in mice lacking αVβ8-TGFβ signaling in the brain. Development. 2014; 141:4489–4499. [PubMed: 25406396]

Bonney S, Harrison-Uy S, Mishra S, MacPherson AM, Choe Y, Li D, Jaminet SC, Fruttiger M, Pleasure SJ, Siegenthaler JA. Diverse Functions of Retinoic Acid in Brain Vascular Development. J Neurosci. 2016; 36:7786–7801. [PubMed: 27445154]

Brault V, Moore R, Kutsch S, Ishibashi M, Rowitch DH, McMahon AP, Sommer L, Boussadia O, Kemler R. Inactivation of the (β)-catenin gene by Wnt1-Cre-mediated deletion results in dramatic brain malformation and failure of craniofacial development. Development. 2001; 128:1253–1264. [PubMed: 11262227]

Breier G, Albrecht U, Sterrer S, Risau W. Expression of vascular endothelial growth factor during embryonic angiogenesis and endothelial cell differentiation. Development. 1992; 114:521–532. [PubMed: 1592003]

Chanda B, Ditadi A, Iscove NN, Keller G. Retinoic acid signaling is essential for embryonic hematopoietic stem cell development. Cell. 2013; 155:215–227. [PubMed: 24074870]

Chen F, Cao Y, Qian J, Shao F, Niederreither K, Cardoso WV. A retinoic acid-dependent network in the foregut controls formation of the mouse lung primordium. The Journal of Clinical Investigation. 2010; 120:2040–2048. [PubMed: 20484817]

Choe Y, Siegenthaler JA, Pleasure SJ. A cascade of morphogenic signaling initiated by the meninges controls corpus callosum formation. Neuron. 2012; 73:698–712. [PubMed: 22365545]

Claxton S, Kostourou V, Jadeja S, Chambon P, Hodivala-Dilke K, Fruttiger M. Efficient, inducible Cre-recombinase activation in vascular endothelium. Genesis. 2008; 46:74–80. [PubMed: 18257043]

Damm K, Heyman RA, Umesono K, Evans RM. Functional inhibition of retinoic acid response by dominant negative retinoic acid receptor mutants. Proc Natl Acad Sci U S A. 1993; 90:2989–2993. [PubMed: 8096643]

Daneman R, Agalliu D, Zhou L, Kuhnert F, Kuo C, Barres B. Wnt/beta-catenin signaling is required for CNS, but not non-CNS, angiogenesis. Proc Natl Acad Sci U S A. 2009; 106:641–646. [PubMed: 19129494]

Darland DC, Cain JT, Berosik MA, Saint-Geniez M, Odens PW, Schaubhut GJ, Frisch S, Stemmer-Rachamimov A, Darland T, D'Amore PA. Vascular endothelial growth factor (VEGF) isoform regulation of early forebrain development. Dev Biol. 2011; 358:9–22. [PubMed: 21803034]

Easwaran V, Pishvaian M, Salimuddin, Byers S. Cross-regulation of beta-catenin-LEF/TCF and retinoid signaling pathways. Curr Biol. 1999; 9:1415–1418. [PubMed: 10607566]

Etchevers HC, Vincent C, Le Douarin NM, Couly GF. The cephalic neural crest provides pericytes and smooth muscle cells to all blood vessels of the face and forebrain. Development. 2001; 128:1059–1068. [PubMed: 11245571]

Fernández-Martínez AB, Jiménez MIA, Cazaña FJL. Retinoic acid increases hypoxia-inducible factor-1α through intracrine prostaglandin E 2 signaling in human renal proximal tubular cells HK-2. Biochimica et Biophysica Acta (BBA)-Molecular and Cell Biology of Lipids. 2012; 1821:672–683. [PubMed: 22306363]

Fernández-Martínez AB, Jiménez MIA, Hernández IS, García-Bermejo ML, Manzano VM, Fraile EA, de Lucio-Cazaña FJ. Mutual regulation of hypoxic and retinoic acid related signalling in tubular proximal cells. The international journal of biochemistry & cell biology. 2011; 43:1198–1207. [PubMed: 21554977]

French CR, Seshadri S, Destefano AL, Fornage M, Arnold CR, Gage PJ, Skarie JM, Dobyns WB, Millen KJ, Liu T, Dietz W, Kume T, Hofker M, Emery DJ, Childs SJ, Waskiewicz AJ, Lehmann OJ. Mutation of FOXC1 and PITX2 induces cerebral small-vessel disease. J Clin Invest. 2014; 124:4877–4881. [PubMed: 25250569]

Green M. The developmental effects of congenital hydrocephalus (ch) in the mouse. Dev Biol. 1970; 23:585–608. [PubMed: 5500588]

Gruneberg H. Congenital hydrocephalus in the mouse, a case of spurious pleiotropism. Journal of Genetics. 1943:1–21.

Haigh JJ, Morelli PI, Gerhardt H, Haigh K, Tsien J, Damert A, Miquerol L, Muhlner U, Klein R, Ferrara N, Wagner EF, Betsholtz C, Nagy A. Cortical and retinal defects caused by dosage-dependent reductions in VEGF-A paracrine signaling. Developmental Biology. 2003; 262:225–241. [PubMed: 14550787]

Haldipur P, Gillies G, Janson OK, Chizhikov VV, Millen KJ. Mesenchymal Foxc1 non-autonomously controls cerebellar development through SDF1α-CXCR4 maintenance of radial glial cells. Int J Dev Neurosci. 2015; 47:34.

Haldipur P, Gillies GS, Janson OK, Chizhikov VV, Mithal DS, Miller RJ, Millen KJ. Foxc1 dependent mesenchymal signalling drives embryonic cerebellar growth. Elife. 2014:3.

Halfter W, Dong S, Yip Y, Willem M, Mayer U. A critical function of the pial basement membrane in cortical histogenesis. J Neurosci. 2002; 22:6029–6040. [PubMed: 12122064]

Harrison-Uy SJ, Pleasure SJ. Wnt signaling and forebrain development. Cold Spring Harb Perspect Biol. 2012; 4:a008094. [PubMed: 22621768]

Hayashi H, Kume T. Forkhead transcription factors regulate expression of the chemokine receptor CXCR4 in endothelial cells and CXCL12-induced cell migration. Biochemical and biophysical research communications. 2008; 367:584–589. [PubMed: 18187037]

Hecht J, Siegenthaler J, Patterson K, Pleasure S. Primary cellular meningeal defects cause neocortical dysplasia and dyslamination. Ann Neurol. 2010; 68:454–464. [PubMed: 20976766]

Hellström M, Gerhardt H, Kalén M, Li X, Eriksson U, Wolburg H, Betsholtz C. Lack of Pericytes Leads to Endothelial Hyperplasia and Abnormal Vascular Morphogenesis. The Journal of Cell Biology. 2001; 153:543–554. [PubMed: 11331305]

Hogan KA, Ambler CA, Chapman DL, Bautch VL. The neural tube patterns vessels developmentally using the VEGF signaling pathway. Development. 2004; 131:1503–1513. [PubMed: 14998923]

James J, Gewolb C, Bautch V. Neurovascular development uses VEGF-A signaling to regulate blood vessel ingression into the neural tube. Development. 2009; 136:833–841. [PubMed: 19176586]

Jiang X, Iseki S, Maxson R, Sucov H, Morriss-Kay G. Tissue origins and interactions in the mammalian skull vault. Dev Biol. 2002; 241:106–116. [PubMed: 11784098]

Kisanuki YY, Hammer RE, Miyazaki J.-i. Williams SC, Richardson JA, Yanagisawa M. Tie2-Cre Transgenic Mice: A New Model for Endothelial Cell-Lineage Analysis in Vivo. Developmental Biology. 2001; 230:230–242. [PubMed: 11161575]

Le Bras B, Barallobre M-J, Homman-Ludiye J, Ny A, Wyns S, Tammela T, Haiko P, Karkkainen MJ, Yuan L, Muriel M-P, Chatzopoulou E, Breant C, Zalc B, Carmeliet P, Alitalo K, Eichmann A, Thomas J-L. VEGF-C is a trophic factor for neural progenitors in the vertebrate embryonic brain. Nat Neurosci. 2006; 9:340–348. [PubMed: 16462734]

Liang C, Guo S, Yang L. All-trans retinoic acid upregulates VEGF expression in glioma cells in vitro. J Biomed Res. 2013; 27:51–55. [PubMed: 23554794]

Liang C, Guo S, Yang L. Effects of all-trans retinoic acid on VEGF and HIF-1α expression in glioma cells under normoxia and hypoxia and its anti-angiogenic effect in an intracerebral glioma model. Mol Med Rep. 2014; 10:2713–2719. [PubMed: 25201493]

Mackenzie F, Ruhrberg C. Diverse roles for VEGF-A in the nervous system. Development. 2012; 139:1371–1380. [PubMed: 22434866]

Maretto S, Cordenonsi M, Dupont S, Braghetta P, Broccoli V, Hassan AB, Volpin D, Bressan GM, Piccolo S. Mapping Wnt/beta-catenin signaling during mouse development and in colorectal tumors. Proc Natl Acad Sci U S A. 2003; 100:3299–3304. [PubMed: 12626757]

Marin-Padilla M. Early vascularization of the embryonic cerebral cortex: Golgi and electron microscopic studies. Journal of Comparative Neurology. 1985; 241:237–249. [PubMed: 4067017]

Mikels A, Nusse R. Wnts as ligands: processing, secretion and reception. Oncogene. 2006; 25:7461–7468. [PubMed: 17143290]

Molyneaux BJ, Arlotta P, Menezes JRL, Macklis JD. Neuronal subtype specification in the cerebral cortex. Nat Rev Neurosci. 2007; 8:427–437. [PubMed: 17514196]

Mulholland DJ, Dedhar S, Coetzee GA, Nelson CC. Interaction of nuclear receptors with the Wnt/beta-catenin/Tcf signaling axis: Wnt you like to know? Endocr Rev. 2005; 26:898–915. [PubMed: 16126938]

Pagès G, Pouysségur J. Transcriptional regulation of the Vascular Endothelial Growth Factor gene–a concert of activating factors. Cardiovascular Research. 2005; 65:564–573. [PubMed: 15664382]

Prasitsak T, Nandar M, Okuhara S, Ichinose S, Ota MS, Iseki S. Foxc1 is required for early stage telencephalic vascular development. Developmental Dynamics. 2015 n/a-n/a.

Raab S, Beck H, Gaumann A, Yüce A, Gerber H, Plate K, Hammes H, Ferrara N, Breier G. Impaired brain angiogenesis and neuronal apoptosis induced by conditional homozygous inactivation of vascular endothelial growth factor. Thromb Haemost. 2004; 91:595–605. [PubMed: 14983237]

Rosselot C, Spraggon L, Chia I, Batourina E, Riccio P, Lu B, Niederreither K, Dolle P, Duester G, Chambon P, Costantini F, Gilbert T, Molotkov A, Mendelsohn C. Non-cell-autonomous retinoid signaling is crucial for renal development. Development. 2010; 137:283–292. [PubMed: 20040494]

Ruberte E, Friederich V, Chambon P, Morriss-Kay G. Retinoic acid receptors and cellular retinoid binding proteins. III. Their differential transcript distribution during mouse nervous system development. Development. 1993; 118:267–282. [PubMed: 8397079]

Sasman A, Nassano-Miller C, Shim KS, Koo HY, Liu T, Schultz KM, Millay M, Nanano A, Kang M, Suzuki T, Kume T. Generation of conditional alleles for Foxc1 and Foxc2 in mice. Genesis. 2012

Siegenthaler J, Ashique A, Zarbalis K, Patterson K, Hecht J, Kane M, Folias A, Choe Y, May S, Kume T, Napoli J, Peterson A, Pleasure S. Retinoic acid from the meninges regulates cortical neuron generation. Cell. 2009; 139:597–609. [PubMed: 19879845]

Siegenthaler JA, Choe Y, Patterson KP, Hsieh I, Li D, Jaminet SC, Daneman R, Kume T, Huang EJ, Pleasure SJ. Foxc1 is required by pericytes during fetal brain angiogenesis. Biol Open. 2013; 2:647–659. [PubMed: 23862012]

Silber HA, Bluemke DA, Ouyang P, Du YP, Post WS, Lima JA. The relationship between vascular wall shear stress and flow-mediated dilation: endothelial function assessed by phase-contrast magnetic resonance angiography. Journal of the American College of Cardiology. 2001; 38:1859–1865. [PubMed: 11738285]

Srinivas S, Watanabe T, Lin CS, William CM, Tanabe Y, Jessell TM, Costantini F. Cre reporter strains produced by targeted insertion of EYFP and ECFP into the ROSA26 locus. BMC Dev Biol. 2001; 1:4. [PubMed: 11299042]

Stenman JM, Rajagopal J, Carroll TJ, Ishibashi M, McMahon J, McMahon AP. Canonical Wnt signaling regulates organ-specific assembly and differentiation of CNS vasculature. Science. 2008; 322:1247–1250. [PubMed: 19023080]

Strong LH. The early embryonic pattern of internal vascularization of the mammalian cerebral cortex. The Journal of Comparative Neurology. 1964; 123:121–138. [PubMed: 14199263]

Stubbs D, DeProto J, Nie K, Englund C, Mahmud I, Hevner R, Molnár Z. Neurovascular Congruence during Cerebral Cortical Development. Cerebral Cortex (New York, NY). 2009; 19:i32–i41.

Tsai S, Bartelmez S, Heyman R, Damm K, Evans R, Collins SJ. A mutated retinoic acid receptor-alpha exhibiting dominant-negative activity alters the lineage development of a multipotent hematopoietic cell line. Genes Dev. 1992; 6:2258–2269. [PubMed: 1334022]

Vallon M, Chang J, Zhang H, Kuo CJ. Developmental and pathological angiogenesis in the central nervous system. Cellular and Molecular Life Sciences. 2014; 71:3489–3506. [PubMed: 24760128]

Vasudevan A, Long JE, Crandall JE, Rubenstein JLR, Bhide PG. Compartment-specific transcription factors orchestrate angiogenesis gradients in the embryonic brain. Nat Neurosci. 2008; 11:429–439. [PubMed: 18344991]

Vivatbutsiri P, Ichinose S, Hytonen M, Sainio K, Eto K, Iseki S. Impaired meningeal development in association with apical expansion of calvarial bone osteogenesis in the Foxc1 mutant. J Anat. 2008; 212:603–611. [PubMed: 18422524]

Ward MC, Cunningham AM. Developmental expression of vascular endothelial growth factor receptor 3 and vascular endothelial growth factor C in forebrain. Neuroscience. 2015; 303:544–557. [PubMed: 25943477]

Won C, Lin Z, Kumar P, Li S, Ding L, Elkhal A, Szabó G, Vasudevan A. Autonomous vascular networks synchronize GABA neuron migration in the embryonic forebrain. Nature communications. 2013:4.

Wu J, Hansen JM, Hao L, Taylor RN, Sidell N. Retinoic acid stimulation of VEGF secretion from human endometrial stromal cells is mediated by production of reactive oxygen species. J Physiol. 2011; 589:863–875. [PubMed: 21173077]

Yang D, Baumann JM, Sun YY, Tang M, Dunn RS, Akeson AL, Kernie SG, Kallapur S, Lindquist DM, Huang EJ, Potter SS, Liang HC, Kuan CY. Overexpression of vascular endothelial growth factor in the germinal matrix induces neurovascular proteases and intraventricular hemorrhage. Sci Transl Med. 2013; 5:193ra190.

Zarbalis K, Choe Y, Siegenthaler JA, Orosco LA, Pleasure SJ. Meningeal defects alter the tangential migration of cortical interneurons in Foxc1(hith/hith)mice. Neural Development. 2012; 7:2–2. [PubMed: 22248045]

Zarbalis K, Siegenthaler JA, Choe Y, May SR, Peterson AS, Pleasure SJ. Cortical dysplasia and skull defects in mice with a Foxc1 allele reveal the role of meningeal differentiation in regulating cortical development. Proc Natl Acad Sci U S A. 2007; 104:14002–14007. [PubMed: 17715063]

Zhou Y, Wang Y, Tischfield M, Williams J, Smallwood PM, Rattner A, Taketo MM, Nathans J. Canonical WNT signaling components in vascular development and barrier formation. J Clin Invest. 2014; 124:3825–3846. [PubMed: 25083995]

Highlights

- Cerebrovascular defects in global *Foxc1* mutants precede cerebral hemorrhage.
- Deletion of *Foxc1* from neural crest-lineage recapitulates cerebrovascular defects.
- Reduced meninges-derived retinoic acid (RA) underlies cerebrovascular growth defects.
- RA may suppress WNT inhibitors to promote growth of vessels into neocortex.
- RA may stimulate expression of VEGFA to promote growth of cerebral vessels.

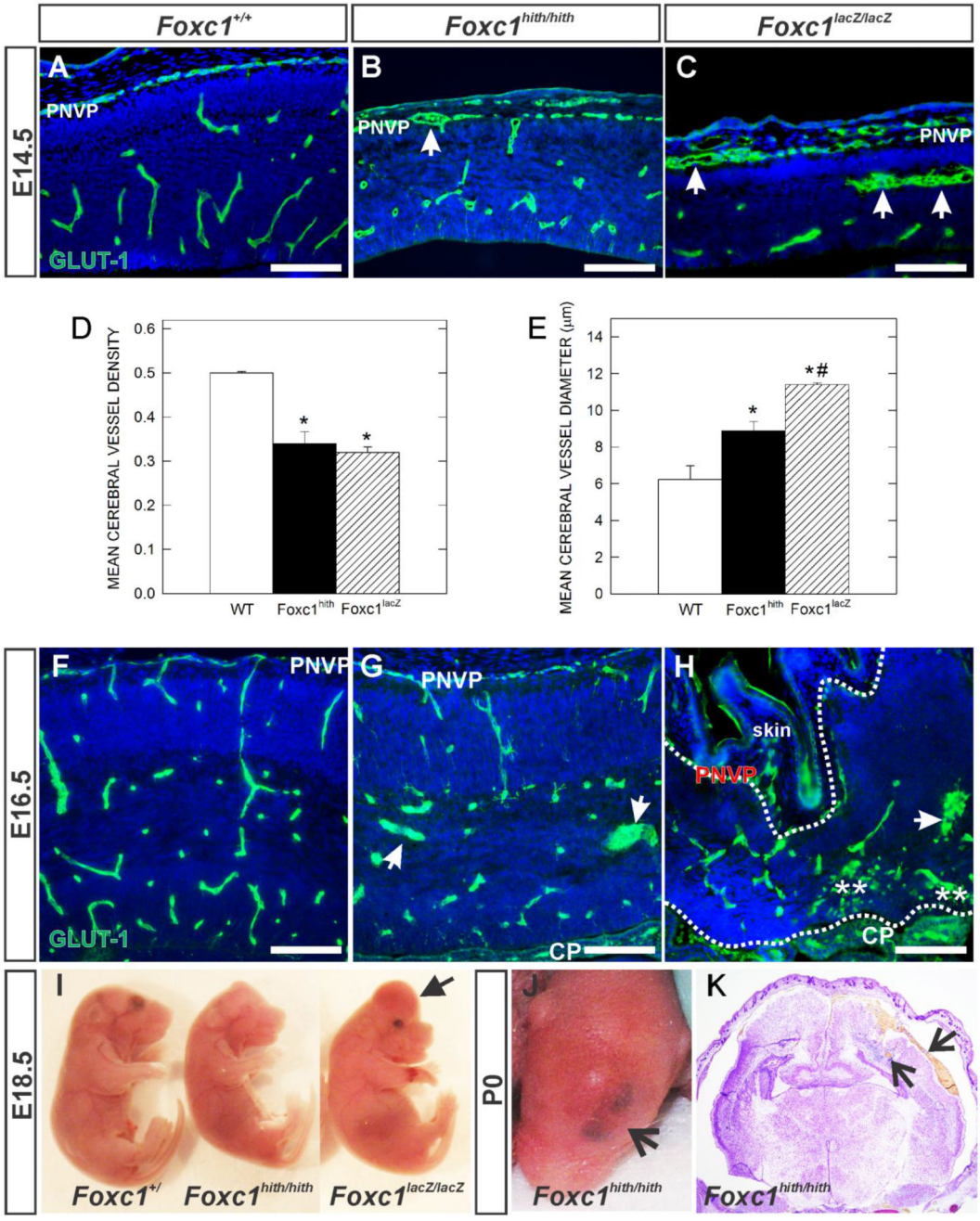

Figure 1.

(A-C, F-H) Immunohistochemistry of E14.5 and E16.5 neocortex of wildtype (*Foxc1*+/+) and *Foxc1* mutants (*Foxc1*$^{hith/hith}$ and *Foxc1*$^{lacZ/lacZ}$) labeled with GLUT1, a CNS blood vessel marker and DAPI. Arrows indicate enlarged, dysplastic vessels. PNVP: Peri-neural vascular plexus. (D, E) Graphs depict quantification of average vessel density (n=3) and vessel diameter (n=4) of E14.5 cerebral vasculature in wildtype (WT), *Foxc1* hypomorph (Foxc1^{hith}) and knockout (Foxc1^{lacZ}) animals. * indicate significant difference from wildtype ($p<0.05$) and *# indicates significant difference from wildtype and Foxc1^{hith}

($p<0.05$). (I) E18.5 embryos harvested from wildtype and *Foxc1* mutants showing forebrain hemorrhage in $Foxc1^{lacZ/lacZ}$ mutant. (J) Postnatal day (P) 0 $Foxc1^{hith/hith}$ mutant showing a characteristic bruise in the head. (K) $Foxc1^{hith/hith}$ coronal section of the brain showing hemorrhage in cerebral cortex (arrow). Scale bars = 100 μm.

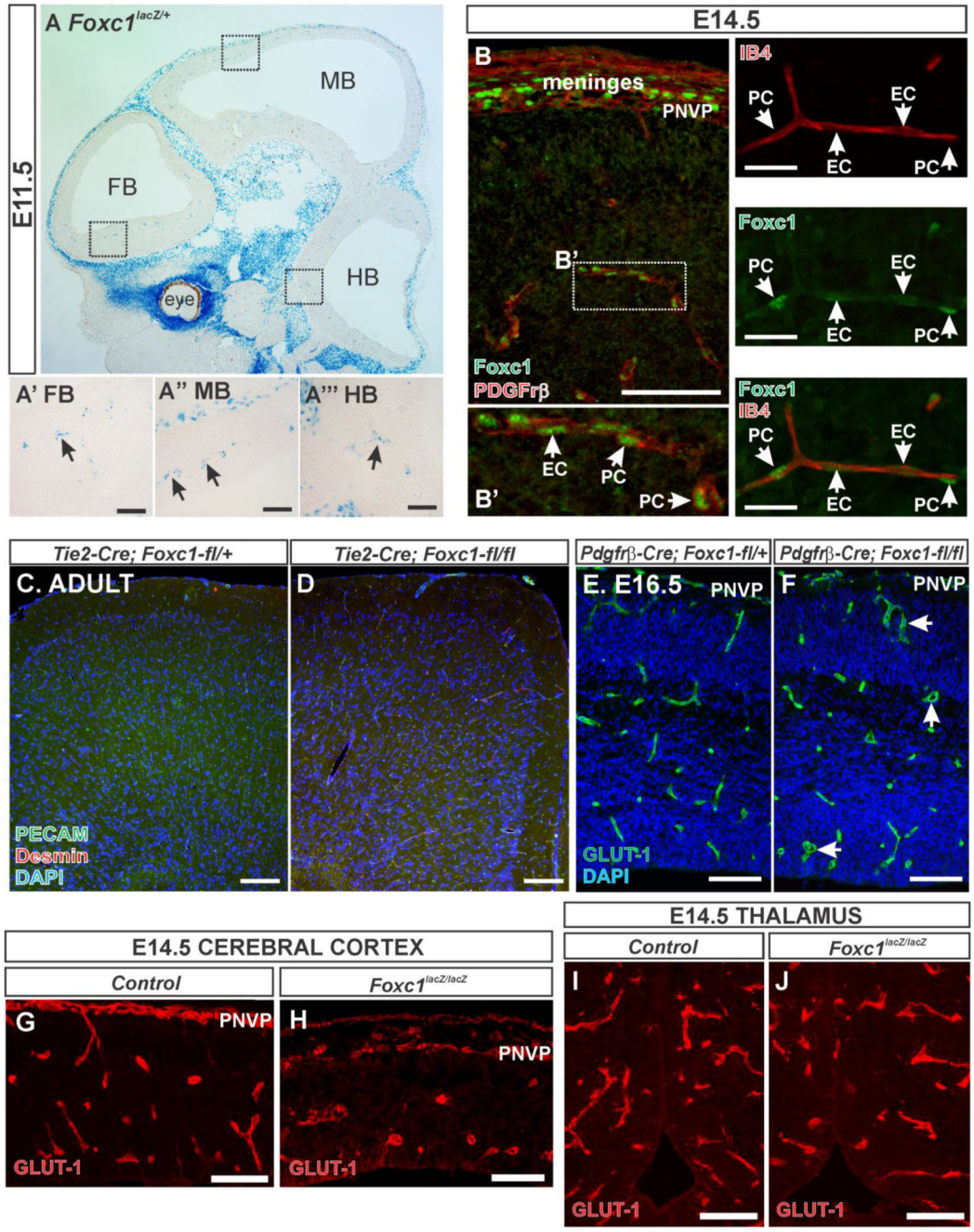

Figure 2.

(A) β-galactosidase (β-gal) activity reflecting Foxc1 expression in a sagittal section of an E11.5 whole head of a *Foxc1*$^{lacZ/+}$ embryo. Boxed areas in (A) are provided as high magnification images of β-gal+ cells in the (A') forebrain, (A") midbrain and (A"') hindbrain. (B) Foxc1 (green) and PDGFrβ (red) immunostaining of E14.5 cerebral cortices and overlying PNVP and meninges. Boxed area in (B) is shown at higher magnification in (B') depicting Foxc1 protein expression endothelial cells (EC) and pericytes (PC) (PDGFrβ + cells). (C) Foxc1 (green) and IB4 (red) immunostaining of E14.5 cerebral vessel. Arrows

indicate Foxc1+ cells, C' and C" depict individual channels. (D) *Tie2-Cre; Foxc1-fl/+* and (E) *Tie2-Cre; Foxc1-fl/fl* adult mice immunostained with PECAM (green) which labels blood vessels and desmin (red) which labels smooth muscle cells and pericytes. Images of E16.5 (F) control- *Pdgfrβ-Cre; Foxc1-fl/+* and (G) mutant *Pdgfrβ-Cre; Foxc1-fl/fl* embryos immunostained with GLUT1 (green) to label blood vessels. Arrowheads in (G) indicate dilated blood vessels. High-magnification images of E14.5 (H-I) cerebral cortex and (J-K) thalamus blood vessels (labeled with GLUT1 in red) from control and $Foxc1^{lacz/lacz}$ mutants. Scale bars = 200 μm (A), 50 μm (A', A", A"', C, C', C"), 100 μm (B, D-K).

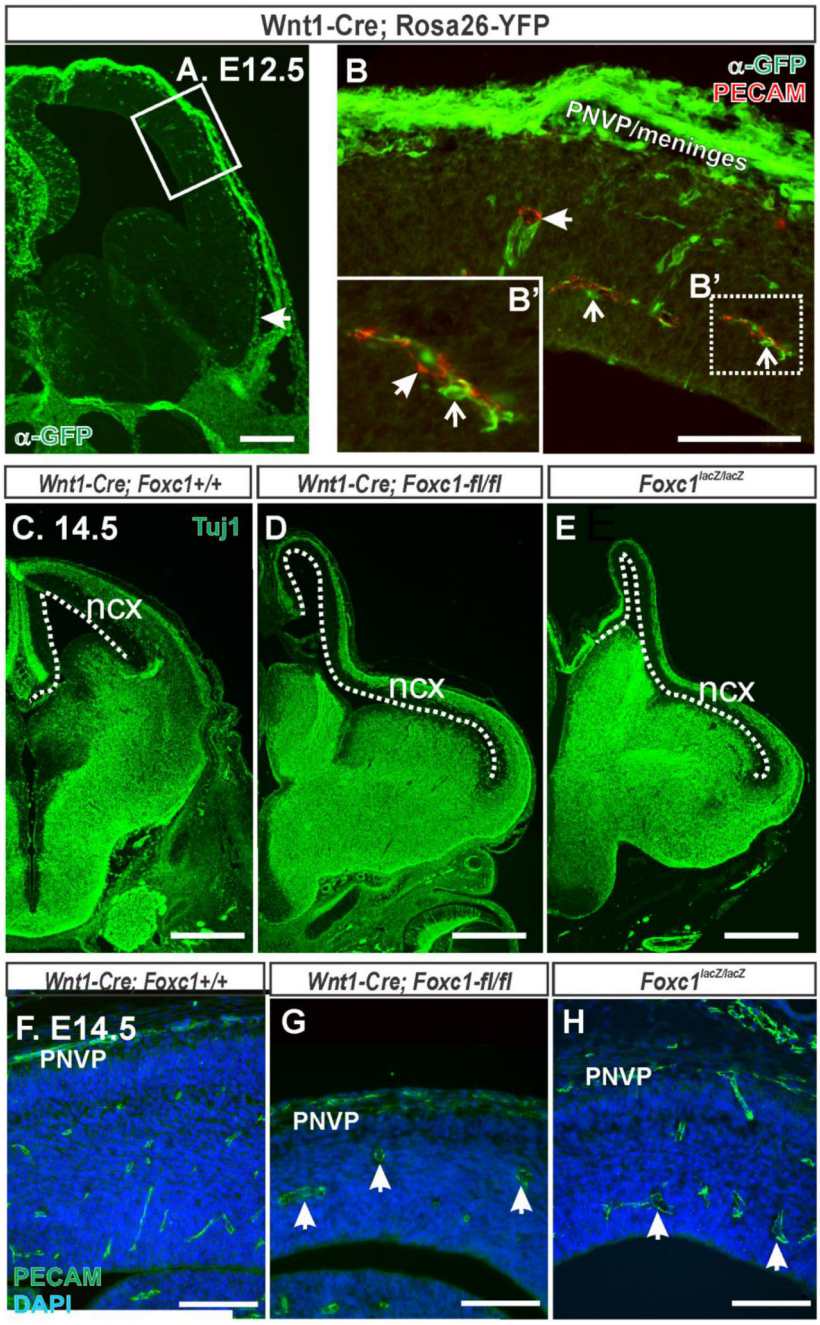

Figure 3.

(A) Low magnification image at the level of the telencephalon of E12.5 *Wnt1-Cre; Rosa26-YFP*, YFP signal (green) indicates *Wnt1-Cre* recombined cells. Box highlights area shown at higher magnification in B. (B) Higher magnification image of the neocortex and overlaying mesenchyme in an E12.5 *Wnt1-Cre; Rosa26-YFP* immunolabeled with PECAM (red). YFP + cells were apparent in the PNVP and meninges. Closed arrows depict PECAM+/YFP− blood vessel and open arrows depict YFP+ perivascular pericytes in B and B'. E14.5 embryonic brains from (C) *Wnt1-Cre;Foxc1+/+*, (D) *Wnt1-Cre;Foxc1-fl/fl and* (E)

Foxc1$^{lacZ/lacZ}$ immunostained with Tuj1 (green) which labels young neurons. Dashed line outlines length of neocortex (ncx). E14.5 neocortex from (F) *Wnt1-Cre;Foxc1+/+,* (G) *Wnt1-Cre;Foxc1-fl/fl,* and (H) *Foxc1*$^{lacZ/lacZ}$ immunolabled with PECAM. Arrows in G, H indicate dilated cerebral vessels. Scale bars = 200 μm (A), 500 μm (C-E), 100 μm (B,F-H).

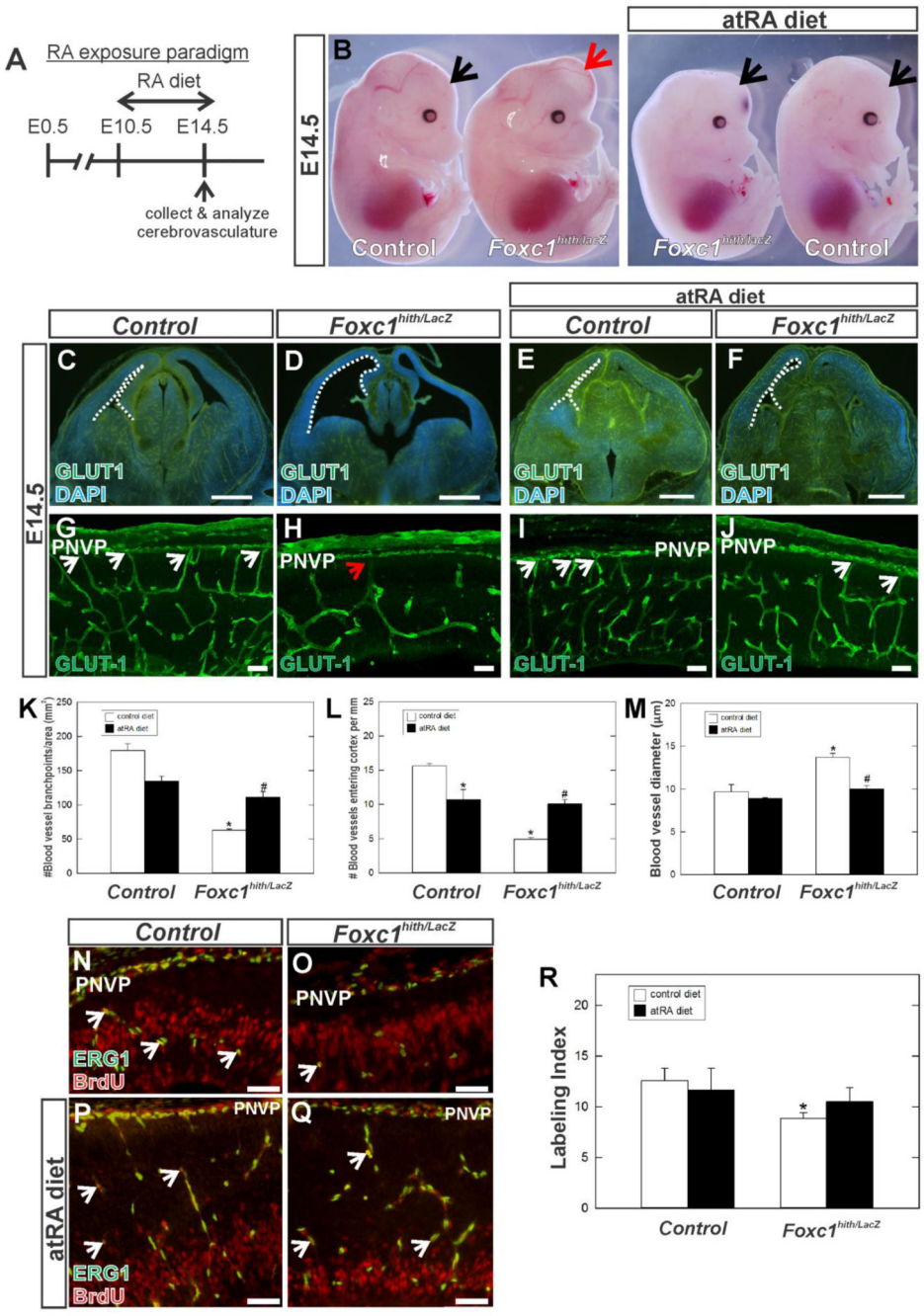

Figure 4.

(A) Schematic depicting atRA diet exposure paradigm. (B) E14.5 non-treated and atRA treated control and *Foxc1*$^{hith/lacz}$ mutant whole embryos. Arrows indicate cerebral hemispheres. (C-J) Low magnification (C-F) images of GLUT1 immunohistochemistry on E14.5 coronal brain sections at the level of the forebrain. Higher magnification images (G-J) of GLUT1 in the neocortex highlight the morphology of the cerebrovasculature. Arrows indicated PNVP-derived vessels at their entry point in the cerebral wall. (K-M) Quantification of vessel branch points, number of blood vessels growing into the cortex from

the PNVP and vessel diameter in untreated (n=3) and atRA treated control (n=3) and *Foxc1*$^{hith/lacZ}$ mutants (n=3). Asterisks indicate statistically significant difference ($p<0.05$) from non-atRA treated condition. Hashtag (#) indicates a statistically significant difference ($p<0.05$) from a non-atRA treated *Foxc1* mutant. (N-Q) Immunohistochemistry of E14.5 cerebral cortex from non-treated (N, O) and atRA-treated (P, Q) wildtype and *Foxc1*$^{hith/lacz}$ mutant labeled with endothelial cell nuclear marker ERG1 and BrdU which labels cells in S phase. Arrows indicate ERG1+/BrdU+ cells. (R) Quantification of endothelial cell proliferation (Labeling Index) in untreated (n=4) and atRA control (n=4) and mutants (n=4). Asterisk indicates statistically significant difference ($p<0.05$) from non-atRA treated control. Scale bars = 500 μm (C-F), 50 μm (G-J), 100μm (N-Q).

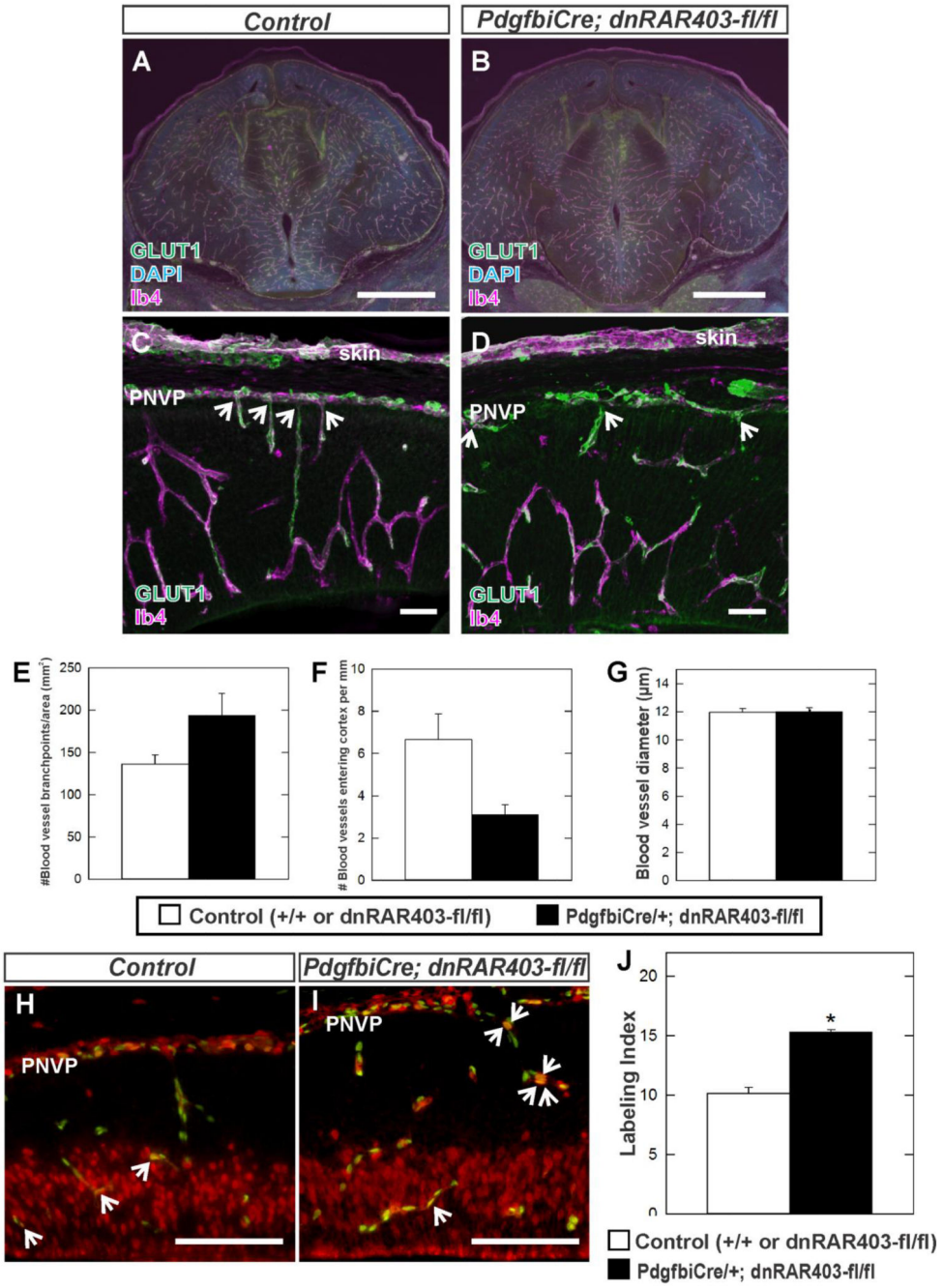

Figure 5.

(A-D) Immunohistochemistry of E14.5 coronal brain sections at the level of the forebrain (A, B) and in the neocortex (C, D) labeled with GLUT1 (green) and IB4 (cyan) from control and *Pdgfbi-Cre;dnRAR403-fl/fl* mutant samples. (E-G) Quantification of vessel branch points, number of blood vessels growing into the cortex from the PNVP and vessel diameter in control (n=3) and *Pdgfbi-Cre;dnRAR403-fl/fl* (n=3). Arrows in C and D indicate PNVP-derived blood vessels. Asterisks indicate statistically significant difference ($p<0.05$) from control. Immunohistochemistry of E14.5 cerebral cortex from (H) control and (I) *Pdgfbi-*

Cre; dnRAR403-fl/fl mutant labeled with endothelial cell nuclear marker ERG1 (green) and BrdU (red) which labels cells in S phase. Arrows indicate ERG1+/BrdU+cells. (J) Quantification of endothelial cell proliferation (Labeling Index) in control (n=3) and *Pdgfbi-Cre;dnRAR403-fl/fl* mutants (n=3). Asterisk indicates statistically significant difference ($p<0.05$) from control. Scale bars = 1000 μm (A-B), 50 μm (C, D), 100 μm (H, I).

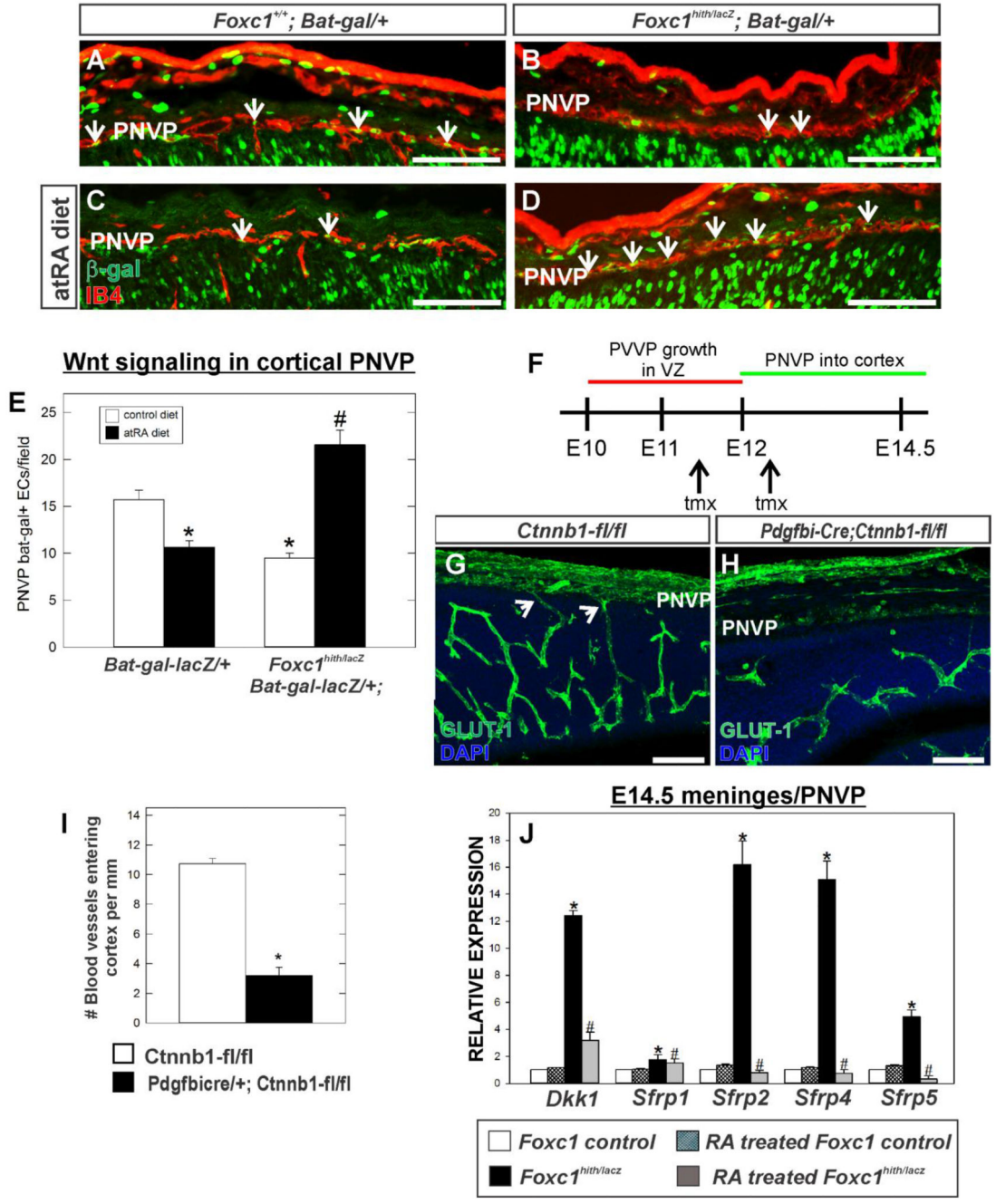

Figure 6.

(A-D) Immunolabeling for β-galactosidase (β-gal) (green) and IB4 (red) of E14.5 coronal brain sections showing PNVP of the cerebral cortex from *Foxc1*$^{+/+}$ and *Foxc1*$^{hith/lacZ}$ (*Foxc1*$^{h/l}$) carrying the WNT reporter transgene, *Bat-gal-LacZ.* (E) Quantification of Bat-gal + endothelial cells in PNVP per 20x field (n=3). Arrows indicate Bat-gal+/IB4+ endothelial cells. Asterisks indicate statistically significant decrease ($p<0.05$) from non-atRA control and hashtag (#) indicates a statistically significant increase ($p<0.05$) from a non-atRA treated control. (F) Approximate timeline PVVP and PNVP growth in the neocortex and

timing of tamoxifen (tmx) injections for *Pdgfbi-Cre;Ctnnb1-flox* experiment. (G,H) E14.5 neocortex labeled with GLUT-1 from control (*Ctnnb1-fl/fl*) and mutant (*Pdgfbi-Cre;Ctnnb1-fl/fl*). Arrows indicate PNVP-derived vessels entering cerebral wall. (I) Quantification of number of blood vessels entering cerebral cortex from PNVP. Asterisks indicate statistically significant difference ($p<0.05$; n=3) from control. (J) Graph depicts gene expression of WNT inhibitors in E14.5 telencephalic meninges/PNVP from atRA-treated control (n=3) and mutants ($Foxc1^{hith/lacZ}$) (n=3) relative to non-atRA treat control (n=3). Asterisks indicate statistically significant difference ($p<0.05$) from non-RA treated control. Hashtag (#) indicates statistically significant difference ($p<0.05$) from non-atRA $Foxc1^{hith/lacZ}$ mutant sample. Scale bars = 100 μm.

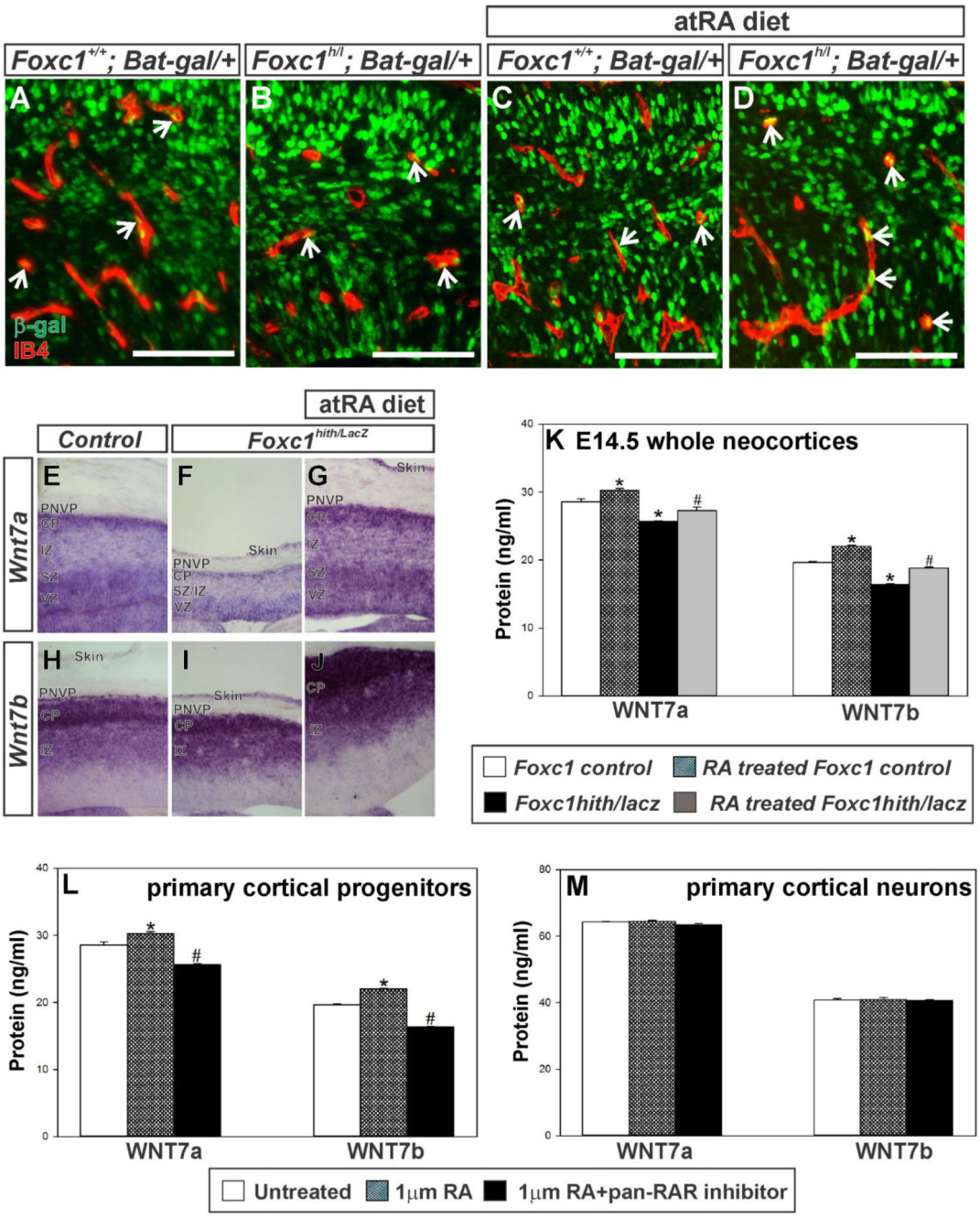

Figure 7.

(A-D) β-galactosidase (β-gal) (green) and IB4 (red) labeling of E14.5 coronal brain sections depicting the intracortical vasculature from *Foxc1*$^{+/+}$ and *Foxc1*$^{hith/lacZ}$ (*Foxc1*$^{h/l}$) carrying the WNT reporter transgene, *Bat-gal-LacZ.* (E-J) In situs of *Wnt7a* and *Wnt7b* on E14.5 wildtype and *Foxc1*$^{hith/lacZ}$ mutant untreated or exposed to atRA from E10-E14.5. CP: cortical plate, IZ: intermediate zone, SZ: subventricular zone, VZ: ventricular zone. (K) WNT7A and WNT7B protein levels in E14.5 cortical lysates from non-untreated (n=3) and atRA treated control (n=3) and mutants (*Foxc1*$^{hith/lacZ}$) (n=3) quantified via ELISA. (L, M)

WNT7A and WNT7B protein expression in lysates from non-treated (n=3), atRA-treated (n=3) and atRA+pan-RAR (n=3) antagonist treated cultured cortical progenitors (L) and neurons (N). Asterisks indicate statistically significant difference ($p<0.05$) from non-RA treated control cells. Hashtag (#) indicates statistically significant difference ($p<0.05$) from atRA treated cells. Scale bars = 100 μm.

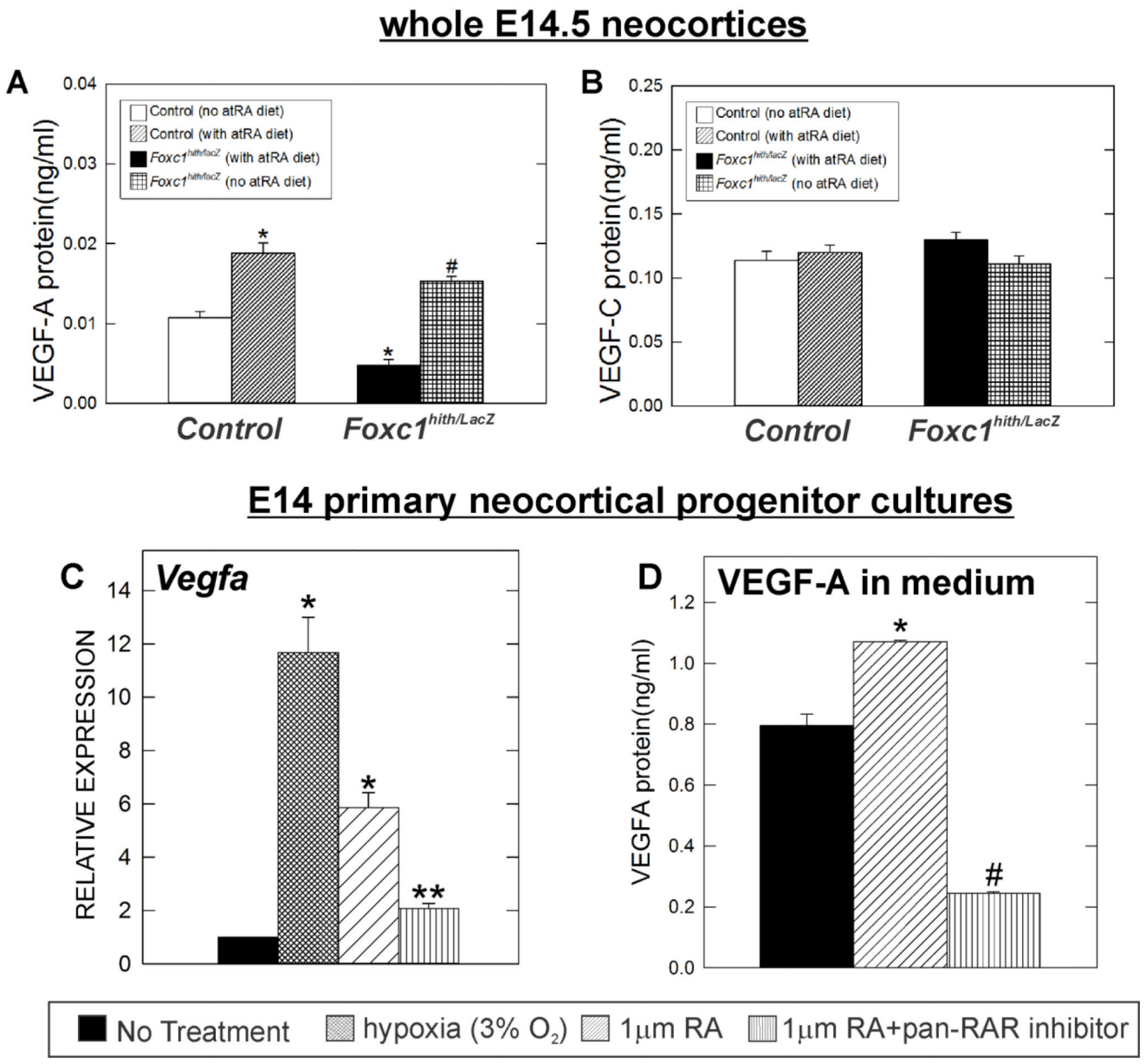

Figure 8.

(A) VEGF-A and (B) VEGF-C protein levels in E14.5 cortical lysates from non-treated (n=3) and atRA treated control (n=4) and mutants (*Foxc1*$^{hith/lacZ}$) (n=3) quantified via ELISA. Asterisks indicate statistically significant difference ($p<0.05$) from non-RA treated control (n=4). Hashtag (#) indicates statistically significant difference ($p<0.05$) from both non-RA treated control and *Foxc1*$^{hith/lacZ}$ mutant samples. (C) *Vegfa* gene expression in hypoxia (n=3), atRA (n=3) or atRA+pan-RAR antagonist (n=3) treated E14 cortical progenitor cells relative to *Vegfa* expression of control (untreated E14 cortical progenitor cells) (n=3) measured by real time-PCR. (D) VEGF-A protein levels in conditioned medium collected from control (untreated) (n=3), atRA treated (n=3) and RA+pan-RAR antagonist (n=3) treated mouse E14 cortical progenitor cells.

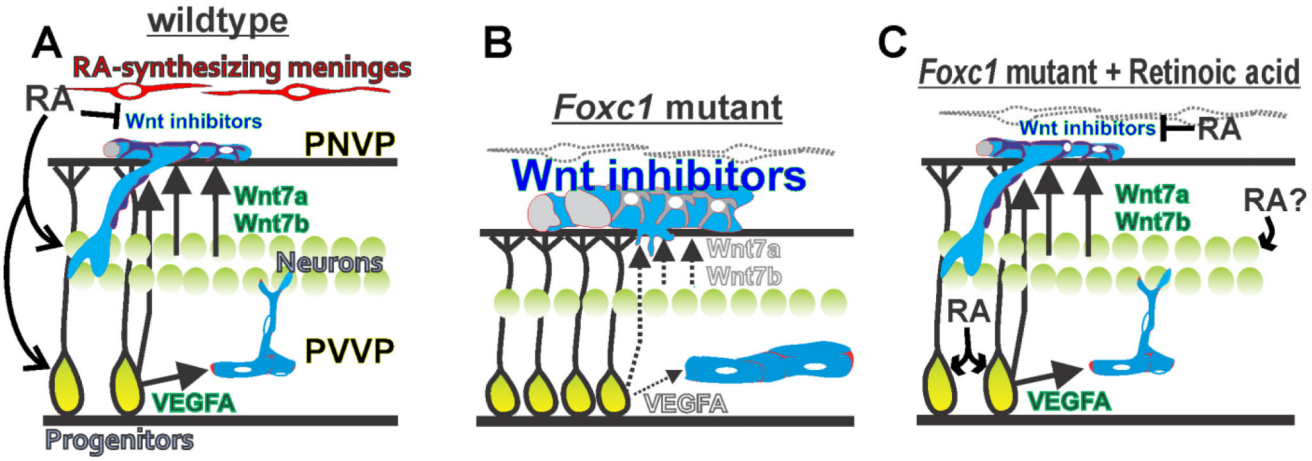

Graphical abstract

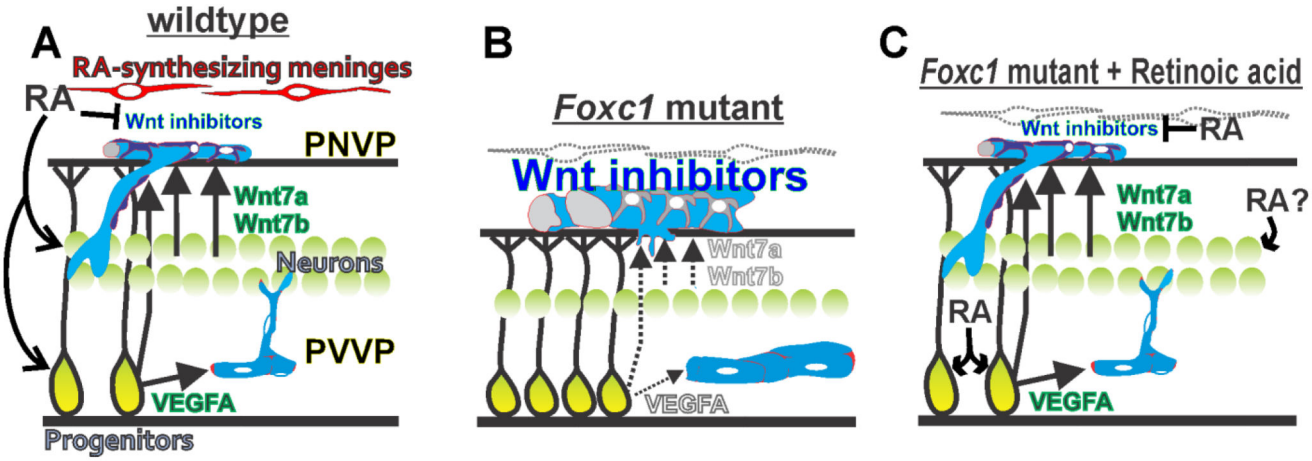

Figure 9.

Hypothetical model of origin of cerebrovascular defects in *Foxc1* mutants (A) Meningeal-derived RA stimulates VEGF-A from progenitors and WNT7a/b from progenitors and neurons to ensure adequate growth of the PVVP and PNVP into the cerebral wall. Expression of Wnt inhibitors is suppressed in the PNVP by meningeal-derived RA. (B) In *Foxc1* mutants that lack meningeal derived RA to the neocortex, diminished VEGF-A expression reduces elaboration of vessels within the neocortex (periventricular vascular plexus or PVVP). Also, reduced numbers of WNT7a/7b-producing neurons, reduced release of WNT7a/7b protein from neocortical progenitors and increased expression of WNT inhibitors in the meninges, prevent adequate growth PNVP-derived vessels into the neocortex. (C) Exogenous treatment of *Foxc1* mutants with RA 1) improves neuron generation and thus production of angiogenic WNT ligands that can signal ‘up’ to the PNVP

2) blocks Wnt inhibitor expression in the meninges 2) acts directly on progenitors and, possibly, neurons to stimulate adequate VEGF-A,WNT7A and WNT7B production for growth of vessels within the neocortex.